Ocean eddies

A. S. Monin and G. M. Zhikharev

P. P. Shirshov Institute of Oceanography of the Academy of Sciences of the USSR
Usp. Fiz. Nauk **160**, 1–47 (May 1990)

The theory and empirical data for three classes of ocean eddies are summarized: 1) gigantic anticyclonic gyres; 2) meanders, rings, and synoptic eddies in the open ocean; and, 3) mesoscale eddies (lenses of foreign waters and rotating cells of forced convection). A number of new results obtained in the last few years are reported: linear and nonlinear instability of gigantic gyres, the Hamiltonian formalism for Rossby-Blinova waves, an eddy-resolving model of global ocean circulation, the discovery of deep mesoscale lenses of foreign waters, and the general prevalence of rotating cells of forced convection in the upper layer of the ocean.

INTRODUCTION

The theory of vortices in liquids and gases dates back to the work of H. Helmholtz in 1958,[1] in which he studied the equation for the curl $\Omega = \nabla \times v$ of the velocity field v in an ideal homogeneous liquid

$$\mathrm{helm}\,\boldsymbol{\Omega} \equiv \frac{d\boldsymbol{\Omega}}{dt} - (\boldsymbol{\Omega}\nabla)\,\mathbf{v} + \boldsymbol{\Omega}\,\mathrm{div}\,\mathbf{v} = 0, \qquad (1)$$

where helm is the *helmholtzian*, linear (tensor) hydrodynamic operator, introduced by A. A. Fridman[2] (the equality helm $A = 0$ means that the vector field A is *frozen-in* in a moving liquid: Each vector line of the field always consists of one and the same particles of liquid and the intensities of the vector tubes do not change with time; according to Ref. 3 all frozen-in fields with a fixed velocity field v form a Lie algebra with the commutator $[\mathbf{A}_1\mathbf{A}_2] = (\mathbf{A}_1\nabla)\mathbf{A}_2 - (\mathbf{A}_2\nabla)\mathbf{A}_1)$. The classical problem is to solve Helmholtz's equation (1) for an incompressible liquid (div $v = 0$) with the boundary condition that solid walls are impermeable to the liquid $(\hat{v}\cdot\nabla)S = 0$ (where $S = 0$ is the equation of the wall, and the caret denotes the boundary value). There is an extensive literature on the hydrodynamic theory of vortices.

Ocean eddies have specific properties which are usually neglected in the general theory. The three most important neglected properties are probably the effect of the rotation of the planet, the stratification of the ocean, and the frictional stress of the wind on the ocean surface. Rotation with angular velocity ω is a transport motion with vorticity 2ω, so that the absolute vorticity in Eq. (1) is equal to $\Omega + 2\omega$, where now (and below) $\Omega = \nabla \times u$ is the curl of the velocity u of relative motion (relative to the rotating frame of reference).

Stratification is engendered by gravity and, naturally, it has a distinguished direction—the vertical. For this reason large- and mesoscale eddies have quasivertical axes (at least in a thin layer such as an ocean whose thickness H is much less than the radius of the planet; it also determines the large scales $L \gg H$ and the mesoscales $L \gtrsim H$). They are described primarily by the vertical component of the curl of the velocity $\Omega_z + f$, where $\Omega_z = \Delta\psi$ (ψ is the stream function of horizontal motion and Δ is the horizontal Laplacian), and $f = 2\omega_z$ is the inertial frequency (or the Coriolis parameter; $2\pi f^{-1}$ is the pendulum day). On earth the typical values of the Kibel number $\mathrm{Ki} = |\Omega_z| f^{-1}$ (in the equatorial zone the Kibel number must be set equal to $\mathrm{Ki} = \Omega(2\omega)^{-1}$) on large scales are small (owing to the fact that the pressure field in large eddies adjusts to the motion so that the action of horizontal pressure drops balances the Coriolis force; then the motion is said to be *geostrophic*). The smallness of Ki makes it possible to simplify substantially the equations describing large-scale ocean eddies.

In the case of stable stratification of the medium (sufficiently rapid increase in the density ρ of the medium with depth) for vertically adiabatically displaced liquid particles with density anomalies the buoyancy force is a restoring force, and there arises the possibility of development of free vertical oscillations with the *Brunt-Väisälä frequency* $N = (-g\rho^{-1}\partial\rho_*/\partial z)^{1/2}$ (where z is the height, g is the acceleration of gravity, and ρ_* is the potential density, i.e., the density adiabatically reduced to the standard pressure). The propagation of such oscillations in the horizontal direction engenders internal gravity waves with frequencies σ lying in the interval $f < \sigma < \max N(z)$. The scale $L_R = HNf^{-1}$ (the so-called *Rossby radius of deformation*) is the typical horizontal scale of internal ("baroclinic," bounded by stratification) large-scale eddies—cyclones and anticyclones, which generate weather in the atmosphere and in the ocean. For $f \sim 10^{-4}\ \mathrm{s}^{-1}$ in the atmosphere ($H \sim 10$ km, $\max N \sim 2\cdot 10^{-2}\ \mathrm{s}^{-1}$) $L_R \sim 2000$ km and in the ocean ($H \sim 5$ km, $N \sim 10^{-3}\ \mathrm{s}^{-1}$) $L_R \sim 50$ km.

The so-called *potential vorticity*, which combines rotation and stratification, is given by

$$\Omega_* = (\boldsymbol{\Omega} + 2\boldsymbol{\omega})\,\rho^{-1}\nabla\eta \approx (\Omega_z + f)\,\rho^{-1}\,\frac{\partial\eta}{\partial z}\,, \qquad (2)$$

where η is the entropy, so that Ω is, to within a normalization constant, the component of the absolute vorticity in the direction of the "thermodynamic vertical" (the gradient of the entropy $\nabla\eta$; in the ocean, where the salinity s also has an effect, it is better to use the *pseudoentropy* η^*, i.e., the en-

 0038-5670/90/050313-27$01.00

tropy reduced adiabatically and isopycnically to some standard salinity s^*). It is not difficult to prove (see, for example, Ref. 4) that in the case of adiabatic motions the potential vorticity, like the entropy, is conserved in liquid particles, i.e., it satisfies the equation $d\omega_* /dt = 0$ or, as they say, it is the adiabatic *Lagrangian invariant* of the motion.

It turns out that in the description of large- and mesoscale ocean eddies the equation $d\Omega_* /dt = 0$ is the basic equation. It can be simplified by taking into account the facts that 1) the indicated eddies are *quasisolenoidal*, i.e., in them the divergence of the velocity is small compared with the curl (so that neglecting, to a first approximation, the divergence, in particular, the factor ρ^{-1} in Eq. (2) can be dropped); 2) owing to *quasihorizontality* the field η (and other thermodynamic fields) can be divided into the main quasistatic part η_0, which depends only on the depth, and a small deviation from it $\eta' = \eta - \eta_0$, which also depends on the horizontal coordinates and the time; and, 3) because of *quasihydrostaticity* $(\partial\eta_0/\partial z)^{-1}\eta' \approx (\rho_0 N^2)^{-1}\partial p'/\partial z$. From the fact that η and Ω_* are conserved there follows[5] the approximate conservation law

$$\frac{d_h}{dt}\left[\ln(\Delta\psi + f) + \frac{\partial}{\partial z}\frac{1}{\rho_0 N^2}\frac{\partial p'}{\partial z}\right] = 0, \tag{3}$$

where $d_h A/dt = \partial A/\partial t + J(\psi, A)$ is the individual derivative relative to the solenoidal horizontal motion, and $J(\psi, A)$ is a determinant of the derivatives of ψ and A with respect to the horizontal coordinates (Jacobian). In this case p' and ψ are related by the so-called *equation of balance*, i.e., the correspondingly simplified equation for the horizontal divergence of the velocity (see, for example, Ref. 6). This quasisolenoidal approximation is applicable even for mesoscale eddies. However for large-scale eddies outside the equatorial zone an even stronger simplification is applicable—the quasigeostrophic approximation, in which $p' \approx \rho_0 f\psi$, and Eq. (3) is reduced to the elegant form

$$\frac{\partial q}{\partial t} + J(\psi, q) = \Phi, \quad q = f + \mathscr{L}\psi, \quad \mathscr{L} = \Delta + \frac{\partial}{\partial z}\frac{H^2}{L_R^2}\frac{\partial}{\partial z}, \tag{4}$$

where $\mathscr{L}\psi$ is the simplified relative potential vorticity ($\mathscr{L}$ is the analog of the three-dimensional Laplacian); here, the right side Φ, engendered by nonadiabatic factors (primarily turbulent viscosity), is included for generality. To this accuracy the potential vorticity is transported just like the usual vorticity in two-dimensional hydrodynamics.

The largest eddies in the ocean are generated by the friction stress of the wind on the ocean surface. The anticyclonic shear between the trade winds in the tropical zone, which blow westward, and the west-east transport at moderate latitudes creates gigantic ocean gyres around the "centers of action"—subtropical atmospheric anticyclones in the Azores and St. Helen's Island in the Atlantic, the Hawaiian Islands and Easter Island in the Pacific Ocean, and Mauritius in the Indian Ocean; the Antarctic Circumpolar Current (ACPC) is also generated by wind (the calculations in Ref. 7, according to which all these currents are generated predominantly not by the wind, but rather by heating and cooling of waters, are apparently a misinterpretation—according to them in an ocean of incompressible liquid none of the observed currents would exist).

The basic experimental data and theoretical information about large-scale ocean eddies are given in Ref. 9 and in Chapters 7 and 8 of Ref. 8. During the last few years a number of promising new results, deserving the attention and support of physicists, concerning ocean eddies have been obtained. In Refs. 10 and 11 it was established that gigantic gyres are unstable, and disturbances of these gyres are subject to triadic interactions of decompositional and even explosive type. It has been found that synoptic eddies are generated not only by the baroclinic instability of large-scale flows but also by the Helmholtz instability in zones of a tangential discontinuity between large eddies of the same type.[12] A Hamiltonian formalism has been constructed for Rossby-Blinova waves.[13-15] The first eddy-resolving global ocean model has been constructed.[16] Deep mesoscale lenses of foreign waters have been discovered.[17,18] Finally, mesoscale structures of the type of jets of forced convection, apparently engendered by "Ekman pumping" in the field of the curl of the wind stress on the surface of the ocean, have been discovered in many regions.[19]

I. OCEAN GYRES

1. FACTUAL DATA

The general notions about the average quasistationary global ocean surface circulation were formed based on observations of floating bottles, drifting of vessels, and direct measurements of the velocity of currents on float-type stations. The most noticeable currents are the gigantic subtropical anticyclonic gyres mentioned in the introduction as well as the cyclonic ACPC. Northward of the subtropical gyres there lie systems of cyclonic motion of waters underneath the corresponding quasistationary atmospheric cyclones: in the Atlantic the cyclonic gyre beneath the Icelandic pressure minimum and beneath the Aleutian minimum in the Pacific Ocean. In the Arctic there is an anticyclonic gyre in the Amerasian Basin. The periods of revolution are equal to about five years for the anticyclonic gyres, nine years for the ACPC, and four years in the Arctic.

As an example Fig. 1 shows the pattern of the currents in the northern half of the Atlantic with the Azores anticyclonic gyre and, northward of 60° N.L., with the Icelandic cyclonic gyre (separated by the polar front from the Labrador and North-Atlantic currents). In particular, the northern continuation of the Gulf Stream, which is especially important for warming Europe, is shown.

Comparison with charts of sea-level winds[22] shows that surface circulations (they actually can be traced to depths of the order of 1500 m) are predominantly wind-generated. Theoretical studies of wind-driven circulation have made it possible to explain the basic properties of ocean gyres observed in the actual data.

A characteristic feature of large-scale ocean gyres is their meridional asymmetry. In western boundary layers the meridional sections of the gyres acquire the character of narrow streams, in which the velocity often reaches values of 1 m/s. The typical examples of such stream flows is the Gulf Stream in the North Atlantic and the Kuroshio current in the Northern Pacific Ocean. In the eastern sections of the gyres, however, there are no such stream flows, and relatively slow southward motions of waters are observed. In Sec. 2 we shall show that this asymmetry is the result of the rota-

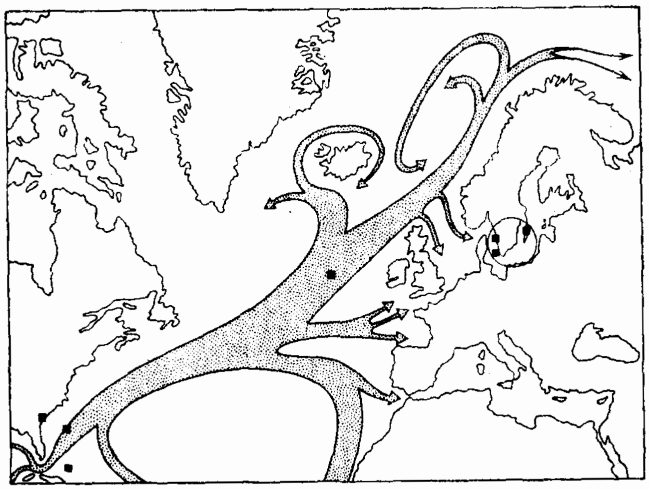

FIG. 1. The Gulf Stream warms Europe.

tion and sphericity of the earth (latitude variation of the Coriolis parameter).

2. WESTWARD INTENSIFICATION

A qualitative explanation of the west-east asymmetry of large-scale ocean gyres was given by H. Stommel in 1948 (see, for example, Ref. 20, Sec. 15 of Ref. 21, and Sec. 46 of Ref. 41). For a qualitative explanation it is sufficient to examine a simplified problem with an ocean of constant depth H, integrated over its entire thickness $0 \geqslant z \geqslant -H$ (the stream function ψ so integrated is called the total stream function), and including in the right side Φ of the equation for the potential vorticity (4) only the effect of "vertical" turbulent viscosity $\mathscr{K}\,\partial^2\Delta\psi/\partial z^2$ (viscosity cannot be neglected, since in the case of stationary flow the integral of the left side of Eq. (4) over any closed horizontal contour is equal to 0, so that the integral of the wind stress contribution must be balanced by the integral of the viscosity contribution). Then for a stationary flow the linearized Eq. (4) integrated over the thickness has the form

$$\frac{fE}{2}\,\Delta\psi + \beta\frac{\partial\psi}{\partial x} = f w_{\rm E},\quad w_{\rm E} = \frac{1}{\rho f}\nabla\times\tau, \tag{5}$$

where x and y are local Cartesian coordinates (the x-axis is oriented eastward and the y-axis is oriented northward); $E = (2\mathscr{K}/f)^{1/2}H^{-1}$ is the *Ekman number* (the relative thickness of the "Ekman" upper layer of the ocean; its absolute thickness $(2\mathscr{K}/f)^{1/2}$ with $\mathscr{K} \sim 200$ cm^2/s is of the order of 20 m); the quantity $\beta = \partial f/\partial y$ is engendered by the rotation and sphericity of the earth (and determines the so-called beta effect); $\omega_{\rm E}$ is the vertical rate of "Ekman pumping" (τ is the wind stress on the surface of the ocean). Neglecting the first term on the left side of Eq. (5) gives the equation of H. Sverdrup (1947), showing that the scale of ψ is $\tau/\rho\beta$ (and the length scale is $f/2\beta$). In these scales Eq. (5) assumes the form $E\Delta\psi + \partial\psi/\partial x = \varphi$, where the right side φ may be assumed to be given. We shall solve this equation in a square basin $0 \leqslant x$ and $y \leqslant 1$ with impermeable shores $\psi = 0$.

We shall represent the functions φ and ψ in the form of series $\Sigma\varphi_n E^n$ and $\Sigma\psi_n E^n$ in powers of the small parameter E; we note, however, that the functions ψ_n, $\partial\psi_n/\partial x$, $\partial\psi_n/\partial y$ cannot be regarded as being of the order of unity, for then we would obtain for ψ_n the first-order equation $\partial\psi_n/\partial x = \varphi_n - \Delta\psi_{n-1}$, and it would be impossible to satisfy the two boundary conditions at $x = 0$ and $x = 1$. For this reason it is necessary to introduce boundary layers with "fast" transverse coordinates $x' = xE^{-1}$ and $x'' = (1-x)E^{-1}$ along the western and eastern shores and the solution must be sought in the form $\psi_n(x,y) + \psi_n'(x',y) + \psi_n''(x'',y)$, where ψ_n, ψ_n' and ψ_n'' differ significantly from zero, respectively, in the open ocean and in the western and eastern boundary layers. The last two requirements mean that the functions ψ_n' must decay rapidly as x' increases while ψ_n'' must decay as x'' increases. For ψ_0'' we obtain the equation $\partial^2\psi_0'/\partial x'^2 + \partial\psi_0'/\partial x' = 0$ which has the decaying solution $\psi_0' = ce^{-x'}$, so that a western boundary layer is formed.

Thus there exists a west-east asymmetry of the gyre with the gyre being intensified in the western section owing to the second term on the left side of Eq. (5), i.e., the β effect.[22]

In an ocean with variable depth the isolines $fH^{-1} = $ const play the role of circles of latitude $f = $ const. Let ds be oriented northward along the tangent to the shoreline. Then a western boundary flow is formed only in the case $\beta' = \partial(fH^{-1})/\partial s > 0$, while an eastern boundary flow is formed if $\beta' < 0$. If, however, the isoline $fH^{-1} = $ const touches the shore at some point, then at that location the sign of β' changes, i.e., under the influence of the bottom relief the boundary flow detaches from the shore.

For a more complete calculation the effect $(fE_{\rm h}/2)\Delta\Delta\psi$ of the "horizontal" turbulent viscosity $\mathscr{K}_{\rm h}$, where $E_{\rm h} = (2\mathscr{K}_{\rm h}/f)^{1/2}L^{-1}$ is the "horizontal" Ekman number, must be included in Eq. (4). Here it can be shown that in the general case the structure of the boundary layers is the same as in the particular case $E_{\rm h} \sim E$. Namely,

1) in the open ocean all three components of the velocity u, v, and w and the variations ζ of the level of the ocean are of the order of E;

2) a surface "Ekman" boundary layer with relative thickness $O(E)$ (i.e., of the order of E), in which $u,v = O(1)$ and $w = O(E)$ forms;

3) a boundary layer of thickness $O(E)$, in which $u,v = O(E)$, $w = O(E^2)$, forms at the bottom;

4) a boundary layer of thickness $O(E^{2/3})$ in which the flow is intensified and in which $u = O(E)$, $v = O(E^{1/3})$, $w = O(E^{2/3})$ and $\zeta = O(E)$.

5) within this layer, just as at the eastern shore, sublayers of thickness $O(E)$ in which upwelling occurs near the shore and in which $u,v = O(E)$ and $\zeta = O(E^2)$, are small while $w = O(1)$ is not small, form; and

6) boundary layers also form at the northern and southern shores.

So far we have ignored inertial effects, described in Eq. (4) by the nonlinear numbers $J(\psi,\Delta\psi)$. They transform the boundary layers into inertial-viscous layers. The theory of these effects was constructed by A. M. Il'in and V. M. Kamenkovich[23] and D. Mur[24] (see also Refs. 4, 8, and 20). In this theory the inertial terms in the dimensionless vorticity equation have the small factor Ki, while the viscous terms have the factor $\mathrm{Ki}^{3/2}\mathrm{Re}^{-1}$, where $\mathrm{Re} = UL_\beta/\mathscr{K}_{\rm h}$ is the Reynolds number of the boundary layer, $U = \tau/(\rho\beta LH)$, and $L_\beta = (U/\beta)^{1/2}$. The solution is sought analogously to the manner described above in the form of a series, but in powers of $\mathrm{Ki}^{1/2}$ and not E. As a result it turns out that for large Re in the southern half of the western shore, where $\partial^2\tau/\partial y^2 > 0$, this layer already vanishes for $\mathrm{Re} \geqslant 10$ (it apparently becomes detached from the shore). For small Re, however, the inertial effects are insignificant.

3. HOMOGENIZATION OF THE POTENTIAL VORTICITY

A volume of fluid in a gigantic gyre can undergo several revolutions before it is carried outside the gyre or approaches the surface of the ocean, where it is subjected to atmospheric action. If the circulation time is sufficiently long, then turbulent mixing tends to homogenize the potential vorticity in the horizontal direction. The condition for such homogenization is the existence of closed contours $\Omega_* = \mathrm{const}$ (or $\psi = \mathrm{const}$).

Homogenization of the relative curl of the velocity within stationary closed contours was first proposed by L. Prandtl and was proved in 1956 by G. Batchelor.[25] P. Rhines and W. Young[26] extended the Prandtl-Batchelor theorem to large-scale flows on a rotating sphere. They proved this theorem approximately, showing based on empirical data that in Eq. (4) outside viscous boundary layers the effects of transport and dissipation q by small-scale turbulence and buoyancy are small compared with the action of synoptic eddies (i.e., transport of q downwards along the gradient ∇q; see the numerical experiments of P. Rhines and W. Holland[27]), and it, in its turn, is small compared with the transport of q by large-scale flows. The latter estimate means that to a first approximation the contours $\psi = \mathrm{const}$ are closed, so that the values of ψ can serve as a "radial" horizontal coordinate (measured from the center of the gyre), and the assertion of the theorem assumes the form $\partial q/\partial\psi \approx 0$.

Rhines and Young employed this theorem to construct gigantic gyres in a three-layer ocean and in a continuously stratified ocean. We shall confine ourselves here to the second case; in addition, exploiting the smallness of Kibel's number, we shall neglect in the expression for q the relative vorticity $\Delta\psi$ compared with the planetary vorticity $f = f_0 + \beta y$. We shall scale the horizontal lengths, the horizontal velocities, the depth, the vertical velocity, the Brunt-Väisälä frequency, and the potential vorticity as L, $U_0 = (w_0 N_0)^{2/3}\beta^{-1/3}$, $H = f_0(\beta N_0)^{-2/3} w_0^{1/3}$, w_0, N_0 and βL, respectively. Then according to the Prandtl-Batchelor theorem

$$q(x, y, z) \equiv y + \frac{\partial}{\partial z} N^{-2} \frac{\partial \psi}{\partial z} = q_0(z), \tag{6}$$

where $q_0(z)$ is an arbitrary function. We shall seek the solution ψ in the bowl-shaped region $0 > z > -D(x,y)$ where $z = 0$ corresponds to the lower boundary of the "Ekman" layer while at the lower boundary of the bowl $z = -D$ there is no motion or variation of the density, i.e., $\psi = \partial\psi/\partial z = 0$. To simplify the analysis we shall confine ourselves to the example of an exponentially stratified ocean (i.e., $N = \mathrm{const}$, in the dimensionless form $N \equiv 1$) and the particular case $q_0 \equiv 1$. Then the solution of Eq. (6) is easily found in the form

$$\psi = \frac{1}{2}(1 - y)(z + D)^2, \tag{7}$$

and the function $D(x,y)$ must be determined from the condition $w = -J(\psi, \partial\psi/\partial z) = w_{\mathrm{E}}$ at $z = 0$. With the help of Eq. (7) it can be put into the form $\partial D^3/\partial x = 6(1-y)^{-1} w_{\mathrm{E}}$, so that $D^3 = 6(1-y)\psi_{\mathrm{E}}$, where ψ_{E} is determined based on w_{E} from Sverdrup's equation. After this the horizontal velocities in the gyre are easily determined: $U = -\partial\psi/\partial y$ and $V = \partial\psi/\partial x$. Thus the Prandtl-Batchelor theorem about the homogenization of the potential vorticity makes it possible to establish the form of a gigantic ocean gyre outside the viscous boundary layers.

McDowell *et al.*[28] calculated the changes in the potential vorticity of large-scale flows $q = \rho_*^{-1} f_1 (\partial\rho_*/\partial z)$ (where ρ_* is the potential density) on meridional sections in the North Atlantic. They employed hydrological data on intermediate water masses, bounded by the isopycnic surfaces $\sigma_* = 26.5$ and $\sigma_* = 27.0$. A region with an almost constant value of $q(y)$, corresponding approximately to the region inside a subtropical anticyclone, was discovered on the sections they constructed. Changes in $q(y)$ were obtained in the numerical model of the circulation of the North Atlantic by P. Rhines and W. Holland;[27] here they also observed a region with constant potential vorticity.

4. INSTABILITY OF OCEAN GYRES

For 40 years theoretical oceanographers have been interested in stationary gigantic gyres, studying their west-east asymmetry and the boundary layer surrounding them. But the question of the possible instability (and, therefore, unrealizability in nature) of stationary gyres was raised only in the last few years in the works of Mirabel' and Monin.[10,11] This time lag can be explained by the fact that the only recently introduced concept of homogenization of the potential vorticity gave a sufficiently simple basis for studying analytically the behavior of disturbances superposed on gigantic gyres. In Ref. 10 such a study was performed for a three-layer ocean and in Ref. 11 it was performed for a continuously stratified ocean. The qualitative results were identical, so that here we shall present only the second case.

So, we superpose on the gyre of Eq. (7) synoptic disturbances with horizontal scales L_{R} ($= \varepsilon L; \varepsilon \ll 1$), vertical scales H, horizontal velocities of the order of $U_R = \gamma U_0$, where γ is the ratio of the typical values of the velocity of the Sverdrup drift flow $w_0 f_0 (\beta H)^{-1}$ and the phase velocity of the Rossby-Blinova waves βL_{R}^2; in order for a gyre, i.e., closed streamlines, to exist γ must not be small, i.e., the contribution of the wind action to the potential vorticity should not be small compared with the contribution of the β effect. In what follows, for simplicity we shall confine ourselves to the particular case $\gamma = 1$, which is adequate for the existence of a gyre, for example, with $\psi_{\mathrm{E}} = 1 - X^2 - Y^2$, vertical velocity of the order of $HL_{\mathrm{R}}^{-1} U_{\mathrm{R}}$ Ki and the time scale $L_{\mathrm{R}} U_{\mathrm{R}}^{-1}$ In the corresponding dimensionless variables the equation for the perturbation of the stream function ψ' will have the form

$$\frac{dq'}{dt} + J(\psi', q') = 0, \quad \frac{d}{dt} = \frac{\partial}{\partial t} + \mathbf{U}(X, Y, z)\nabla, \tag{8}$$

where $q' = \Delta\psi' + \partial^2\psi'/\partial z^2$ is the perturbation of the potential vorticity, and the operators J, ∇, and Δ operate with respect to the "fast" variables (x,y), and the capital letters denote "slow" variables $(X,Y,T) = \varepsilon(x,y,t)$. Here we shall not introduce disturbances of the boundary region D, since the boundary conditions will have the form $w' = 0$ at $z = 0$, $-D$. We shall seek the solution of Eq. (8) in the form of the series $\psi' = \varepsilon\psi_1 + \varepsilon^2\psi_2 + \dots$, and in addition the first approximation will give the solution of the problem of linear instability. It is obtained from the linear equation $dq_1/dt = 0$ with the boundary conditions $(d/dt)\partial\psi_1/\partial z = \mathbf{U}\nabla\psi_1$ at $z = 0$, $-D$ and has the form $\psi_1 = A(X,Y,T)B(z)e^{i\theta} + \text{c.c.}$, where $\theta = k\cdot x - \omega t$ is the "fast" phase, k is the wave vector, and ω is the frequency. Because the coefficients in Eq. (8) are variable the calculation of the amplitude function $B(z)$ and the dispersion relation $\omega = \omega(k)$ is somewhat unwieldy, and we present here only the main results. The dispersion relation is obtained by setting to zero the average Lagrangian:

$$\Lambda \equiv \frac{\omega_r'(0)}{\omega_r(0)} - k\frac{k\omega \operatorname{sh}\chi + \omega_r'(-D)\operatorname{ch}\chi}{k\omega\operatorname{ch}\chi + \omega_r'(-D)\operatorname{sh}\chi} = 0, \qquad (9)$$

where $\chi = kD$ and $\omega_r(z) = \omega - \omega_D(z)$, and in addition $\omega_D = \mathbf{k}\cdot\mathbf{U}(z)$ is the Doppler shift of the frequency. For a normalized zonal phase velocity of the disturbances $c = \omega k_x^{-1}D^{-2}$ Eq. (9) is a quadratic algebraic equation, and the condition that it have complex roots (i.e., linear instability of the main gyre) reduces to the form

$$c_D^2\left(\frac{\chi}{2} - \operatorname{th}\frac{\chi}{2}\right)\left(\frac{\chi}{2} - \operatorname{cth}\frac{\chi}{2}\right) + \frac{1}{4}\operatorname{csch}^2\chi < 0, \qquad (10)$$

where c_D is the normalized value of the Doppler shift of the phase velocity at $z = 0$. Except for the last term this condition is identical to the well-known criterion of the baroclinic instability of stratified flow in the model of E. Eady,[29] in which U is proportional to z and $V = 0$ (here we do not study disturbances with a continuous spectrum, since, according to J. Pedlosky,[30] by analogy to the model of Eady, they do not destroy the stability of the gyre). The region (10) of linear instability in the $\ln|c_D^{(1)}|$, χ plane is shown in Fig. 2 (broken line).

We calculated examples of the dispersion curves $\omega = \omega(k_x)$ of linearly stable waves with $k_y D = 10^{-2}$ for $c_D = -1$ and $c_D = -1/2$. From the form of these curves it may be concluded that such waves are capable of triadic resonance interactions. The so-called adiabatic invariant $\partial\Lambda/\partial\omega$ changes sign on the curves with $c_D = -1$, so that, as is well known, waves with such dispersion curves can form resonance triads with explosive interactions (in such triads the amplitudes A_n of the waves forming them can become infinite over a finite time, which results in "point collapse," i.e., formation of a singularity at some point in space). On

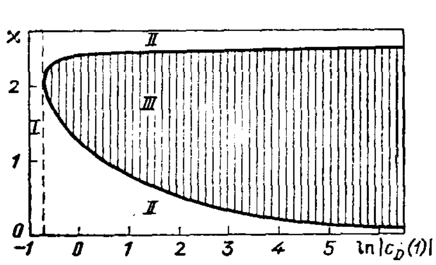

FIG. 2. Diagram of the instability of a gigantic gyre in an exponentially stratified ocean. I, II—regions with decaying and explosive triadic interactions, III—region of linear instability.

the curves with $c_D = -1/2$ the sign of the adiabatic invariant does not change, so that the corresponding waves can form triads with disintegrating interactions.

To construct the equations for the amplitudes $A_n(X,Y,T)$ of waves in a resonance triad

$$\psi_1 = \sum_{n=1}^{3} A_n B_n(z)\, e^{i\theta_n} + \text{к. с.},$$

where the phases satisfy the resonance condition $\theta_1 + \theta_2 = \theta_3$, we shall seek the second approximation in an analogous form

$$\psi_2 = \sum_{n=1}^{3} C_n(X, Y, T, z)\, e^{i\theta_n} + \text{к. с.}$$

Equating in the equations of the second approximation the coefficients of like harmonics we obtain for C_1, C_2, and C_3 inhomogeneous equations with inhomogeneous boundary conditions. The conditions of solvability must hold for these inhomogeneous equations; these conditions reduce to the following canonical form:

$$D_1A_1 = \Gamma I_1^{-1}A_2^*A_3^*, \quad D_2A_2 = \Gamma I_2^{-1}A_1A_3, \quad D_3A_3 = -\Gamma I_3^{-1}A_1A_2, \qquad (11)$$

where D_n are differentiation operators with respect to the "slow" variables $\partial/\partial T - I_n^{-1}[(\partial\Lambda/\partial\mathbf{k})_n \nabla_{x,y}(\partial\Lambda/\partial\mathbf{k})_n]$, and $c_{gn} = -I_n^{-1}(\partial\Lambda/\partial\mathbf{k})_n$ are the group velocities, $I_n = (\partial\Lambda/\partial\omega)_n$ are the values of the adiabatic invariant, and Γ is the three-wave interaction constant, given by the formula

$$\Gamma = (k_{1x}k_{2y} - k_{1y}k_{2x})\Big[(\omega_{r1}(0)\,\omega_{r2}'(0) - \omega_{r2}(0)\,\omega_{r1}'(0)) \times \prod_{n=1}^{3}\omega_{rn}^{-1}(0)\,B_n(0) - (\omega_1\omega_{r2}'(-D) - \omega_2\omega_{r1}'(-D)) \times \prod_{n=1}^{3}\omega_{rn}^{-1}B_n(-D)\Big]. \qquad (12)$$

Methods for solving Eqs. (11) analytically have been developed by V. E. Zakharov.[31]

Observational data show that the instability described here apparently does not destroy gigantic gyres (or, at least, their western intensified sections), but rather it results in quasiperiodic (with periods of the order of several months) transfer of an appreciable fraction of the energy (accessible potential energy) of the gyres into the kinetic energy of "baroclinic" synoptic eddies. This creates autooscillations of the intensity of the gyres and the antiphase collection of synoptic eddies of a relaxational character (since energy is always being pumped in from the outside—from the wind) generated by them. In nature these autooscillations are superposed on quasiregular seasonal oscillations of the general circulation of the atmosphere and ocean (which we neglected here in the theory), which together engender on the gyres with their long (many-year) periods quasirandom sequences of intensified and weakened sections.

As an example Fig. 3 presents graphs (taken from Ref. 9) of oscillations of the kinetic energy density of synoptic eddies at four depths during a 13-month observational experiment POLYMODE in the Atlantic south of the Gulf

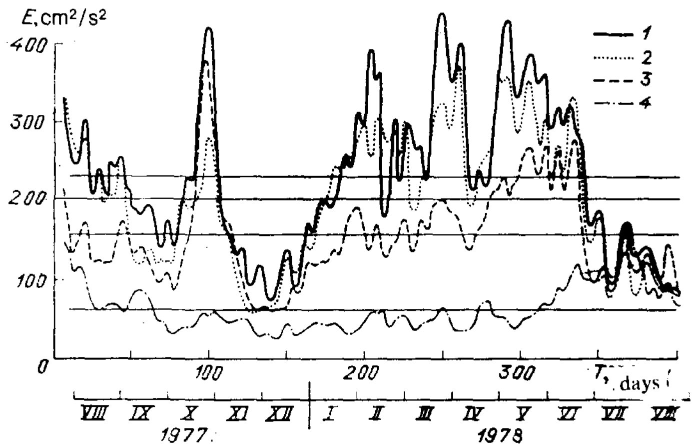

FIG. 3. The kinetic energy of synoptic flows at the levels 100 (1), 400 (2), 700 (3), and 1400 (4) m, averaged over the POLYMODE survey area, as a function of time. The straight lines correspond to the average values of the kinetic energy at four levels.

Stream (see below). We note that the sharp energy minima in the upper layers of the ocean in the periods November–December 1977 and July–August 1978 are clearly unrelated with the phase of the seasonal oscillations; the fact that these minima coincide with the periods of homogenization of energy along the vertical ("barotropization") apparently indicates that the baroclinic instability of large-scale flows plays an important role in the generation of synoptic disturbances.

II. SYNOPTIC EDDIES

5. MEANDERS, RINGS, AND EDDIES

Stream flows meander in the ocean, like rivers do on land. The meandering of the Gulf Stream was the first to be studied and in greatest detail (P. Church (1937);see also the famous book by H. Stommel[32]). This current, which carries warm waters from the Straits of Florida to the southern tip of the Grand Banks of Newfoundland, is 70–90 km wide and extends almost to the bottom; its velocity reaches 3.5 m/s at the ocean surface and decreases rapidly with depth (to 10–20 m/s at depths of 1000–1500 m); the total flow rate is of the order of 0.1 km^3/s. It separates the cold and somewhat fresher water in the north and the warm salty water from the Sargasso Sea in the south (see the temperature section in Fig. 4): at a depth of 300 m the temperature drops across the flow from south to north from 17-18 to 8-9 °C, especially sharply in the north (the "cold wall" of the Gulf Stream). As it passes by Cape Hatteras (35° N.L.) the Gulf Stream moves away from the continental shelf into the open ocean and starts to meander (Fig. 5).

The meanders of the Gulf Stream are 300-400 km long and the swings reach 500 km; they move downstream with speeds of 6-10 cm/s. The Kuroshio current, the ACPC, and other currents meander in an analogous manner. The meandering is caused primarily by baroclinic instability of stream flows and the effect of the bottom relief. With the bottom relief $z = -H + Sy$ and flow with velocity $U(z)$ along the isobaths $y = \text{const}$, the linearized equation (4) for the transverse wave $v \sim \exp[i(kx - \omega t)]$ gives the following dispersion equation:

$$\omega^2 + \left(\frac{fS}{kH} - 2k\bar{U}\right)\omega + k^2\overline{U^2} - \frac{fSU_b}{H} = 0, \qquad (13)$$

where the overbar denotes averaging over the depth and the subscript b denotes the value at the bottom. From here we can see that

1) stationary "topographic" meanders ($\omega = 0$) with wave number $k = (fSU_b/H\overline{U^2})^{1/2}$ are possible;

2) for $U = \text{const}$ ("barotropic" flow) all frequencies ω are real, i.e., all meanders are stable; and,

3) for $U \neq \text{const}$ ("baroclinic" flow) and sufficiently small fS/H the frequencies ω are complex, i.e., the meanders are unstable.

Expanded meanders can separate from the main flow, which in the process reconnects along the shortest path. The detached meanders of rivers on dry land are called oxbows; the flow in them stops, and they gradually become overgrown. The detached meanders of stream flows in the ocean

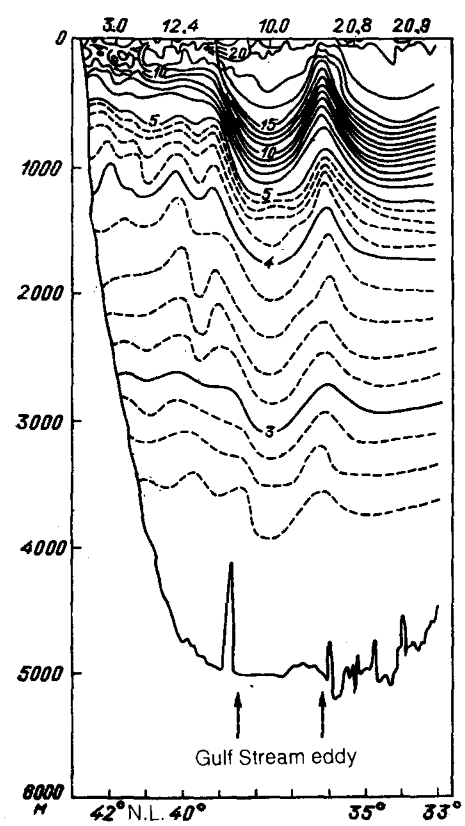

FIG. 4. The temperature distribution (in °C) on the section along 64° 30′ W. L. in April 1960. The section intersects the Gulf Stream and the cyclonic eddy generated by it.

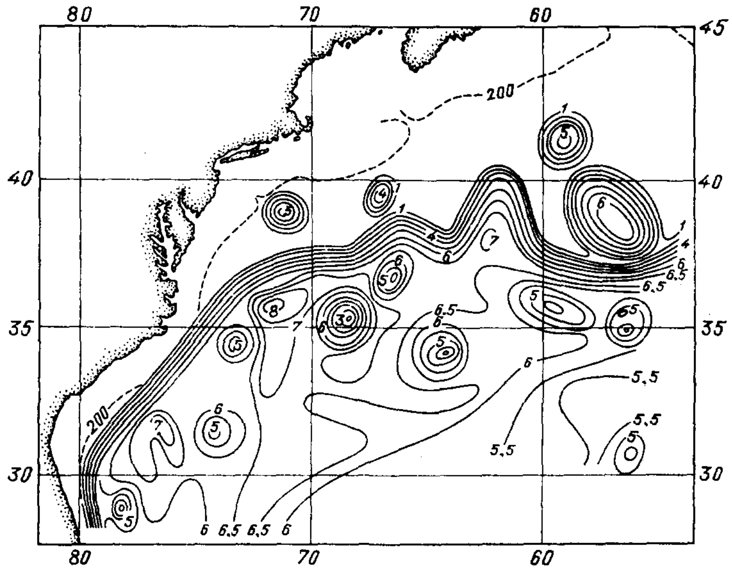

FIG. 5. The topography (in hundreds of meters) of the isothermal surface at 15 °C based on data from bathythermographic, bathythermosaline, and bathometric observations performed in the period from March 15 to July 9, 1975. The extended ribbon-shaped bundle of isothermals is the Gulf Stream. Cold cyclonic eddies can be seen south of the Gulf Stream and warm anticyclonic eddies can be seen north of the Gulf Stream.

behave completely differently: their ends connect and form so-called rings—ring flows, which contain nearly immobile water trapped from the other side of the main flow. Thus cyclonic rings (with counterclockwise flow) containing northern (cold) water form southward of the Gulf Stream and, conversely, anticyclonic rings (with clockwise flow) containing southern (warm) water form northward of the Gulf Stream.

A cold cyclonic ring (latitude of about 36°), which can be traced to depths exceeding 3500 m, can be seen in the temperature section of Fig. 4 to the right of the Gulf Stream (located here at a latitude of about 39°). Four warm and somewhat cold rings of the Gulf Stream can be seen in the map in Fig. 5.

Gulf Stream rings were described by F. Fuglister and L. Worthington (see Ref. 33). Young cyclonic rings have diameters of the order of 200 km, horizontal temperature differences of up to 10–12 °C (which corresponds to differentials of the depths of the isothermal surfaces in the interval 6–17 °C of up to 600–700 m), and orbital velocities of up to 3 m/s in the upper layers of the ocean and of the order of 10 cm/s at depths of 1–2 km, so that spiralling occurs in them. To a lesser extent they penetrate to depths of 3 km and, possibly, even to the bottom. They move westward or southwestward with speeds of the order of 3 cm/s in the upper 700-100 m layer of the ocean, carrying water with them (and serving as unique "incubators" for plankton and organisms of higher trophic levels); at large depths they possibly move through the water in a wave-like fashion (this question requires further study). Their average lifetimes are two to three years (they are absorbed by the Florida current or decay completely), and since five to six such rings are formed every year, in the Sargasso Sea ten to 12 rings can be observed at the same time.

The anticyclonic rings of the Gulf Stream are somewhat smaller (their diameters are equal to 150–200 km), the horizontal temperature differences in them are equal to 9–10° (the differentials of the depths of the isothermal surfaces are 400–500 m), the orbital velocities in their upper layers can exceed 1 m/s, they move westward or southwestward with speeds of the order of 5 cm/s, and they vanish, being absorbed by the Gulf Stream near Cape Hatteras. Their lifetimes are of the order of six months, so that two to four such rings can be observed simultaneously (we note that all young rings can be clearly seen in infrared satellite photographs). The rings of the Kuroshio and other currents have an analogous character (see Ref. 9), but the statistical sample accumulated for them, and especially for the ACPC, is much smaller.

Rising of deep waters (upwelling) should occur along the axes of cyclonic rings (C) and sinking of surface waters (downwelling) should occur in anticyclonic rings (A), so that compensational poloidal circulation should occur in the meridional sections of the rings; see Fig. 6 from Ref. 34. Thus the hydrodynamic model of rings is quite complicated.

Meanders on currents and rings are synoptic disturbances of frontal origin (western boundary flows). It turned out that disturbances on such scales also arise in the open ocean not far from some currents and that such synoptic eddies in the open ocean are quite common and contain a large relative fraction of the kinetic energy of ocean currents. Their discovery was an enormous event in the hydrodynamics of the ocean during the postwar years. They were predicted by the Soviet oceanographer V. B. Shtokman based on analysis of measurements of currents of long periods of time in 1935 in the Caspian Sea, and continued in 1956 in the Black Sea and in 1958 in the North Atlantic.

Indications of intense synoptic variability of currents in the open ocean appeared in the works of other authors also.

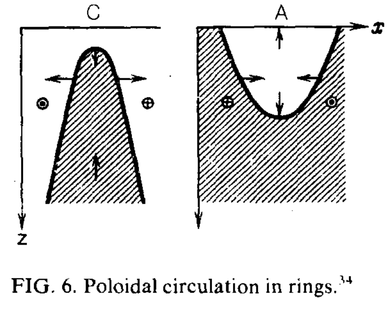

FIG. 6. Poloidal circulation in rings.[34]

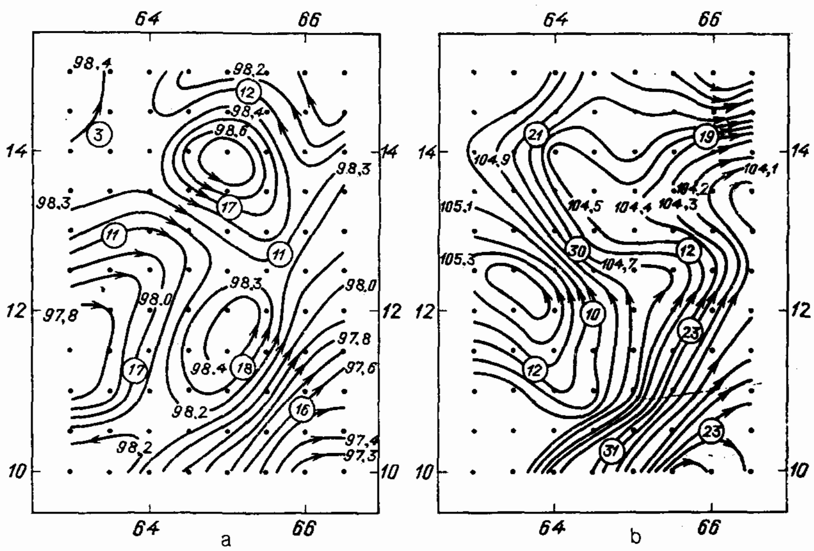

FIG. 7. Geostrophic flows at a depth of 150 m according to data from the first (a; January 21–February 7, 1967) and second (b; March 20–April 6, 1967) hydrological surveys in Poligon-67.

Studies performed by the English oceanographer J. Swallow struck a resonant chord.[35] In 1959–1960 he deployed in the region southwestward of the Bermuda islands neutral-buoyancy floats at depths of 2 and 4 km, and he discovered instead of a weak constant transport of deep waters southward a strong nonstationary oscillatory flow with a period of about 20 days and a wavelength of about 100 km. Analogous results were obtained from flow and temperature measurements by American oceanographers in 1954–1969 in the same region of the Bermuda islands as well as in 1965–1967 northward of the Gulf Stream. K. Wyrtki[36] described temperature oscillations with a wavelength of about 500 km on 44 meridional sections across the North Equatorial Current in the region southwestward of the Hawaiian Islands in the Pacific Ocean in 1964–1965.

To study systematically synoptic flows in the ocean V. B. Shtokman proposed a method for performing long-time measurements over bounded areas of the ocean—so-called survey areas. In addition to hydrological surveys, autonomous floating stations (AFSs) are employed in these survey areas to measure directly the velocities of flows at different levels. In 1967 the Institute of Oceanography of the Academy of Sciences of the USSR organized with the participation of V. B. Shtokman, the first expedition of this kind ("Poligon-67") in the Arabian Sea.[37] The results of calculations of flows based on data from two hydrological surveys, presented in Fig. 7, made it possible to identify for the first time synoptic eddies in the open ocean. The distance a from the center of the eddies to the region with the highest flow velocity was of the order of 100 km, which agrees well with the Rossby radius of deformation L_R, equal to approximately 70 km on the survey area (if a is interpreted as one-fourth the wavelength in the velocity field of the flow, then the wavelength of the disturbance divided by 2π is close to L_R). Estimates of the average (over the survey area) rate of transformation of available potential energy (APE) of a large-scale flow into APE of eddies indicated a stable maximum at depths of 500–600 m.[38] This suggested that the synoptic eddies formed primarily owing to the baroclinic instability of a large-scale flow. However the time interval between two surveys (about two months) was too long for tracing the evolution of the eddies, and in addition the maps of the flows were constructed based on indirect data only.

Poligon-70, conducted by the Institute of Oceanography of the Academy of Sciences of the USSR in February–September 1970 on the southern periphery of the Northern Equatorial Current in the Atlantic Ocean, became an important supplement to Poligon-67.[39] The main observations were conducted on 17 AFSs, in whose region several hydrological surveys were made. The main result of the expedition was the discovery of an anticyclonic eddy, passing directly through the center of the survey area in the direction west-southwest with a speed of about 5 cm/s over a period from the beginning of April to the beginning of July 1970 (Fig. 8). Aside from it, a warm part of one other anticyclone and the frontal region of a cyclone, which drifted immediately behind the first anticyclone, were recorded. The nonstationary velocity field of synoptic eddies was significantly greater in magnitude than the velocity of the weak Northern Equatorial Current. The eddy observed in the survey area had an elliptical shape with a minor semiaxis of about 100 km, which agrees fairly well with the Rossby radius L_R -65 km.[40] Aside from the good agreement of these scales the fact that the eddy was the result of a baroclinic instability was also indicated by the inclination of the axis of the eddy with depth.[41]

American scientists obtained the same results (on a smaller scale) during the MODE (Mid-Ocean Dynamics

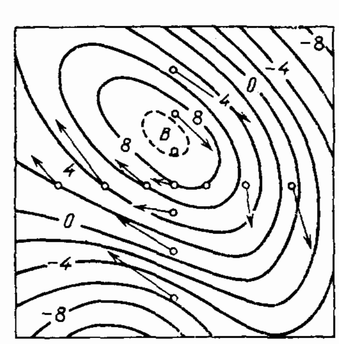

FIG. 8. Map of synoptic flows at a depth of 300 m in the Poligon-70 for May 24, 1970 (according to Yu. M. Grachev and M. N. Koshlyakov).

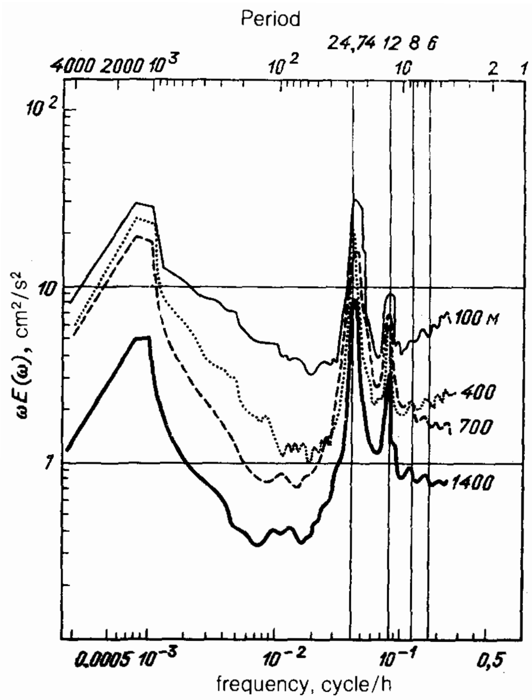

FIG. 9. Frequency spectra of the kinetic energy of flows at the 100, 400, 700, and 1400 m levels according to measurements of flows on the POLYMODE float system.[37] The circular frequency is plotted along the horizontal axis and the product of the spectral density and the frequency is plotted along the vertical axis.

Experiment) experiment in the Sargasso Sea in March–June 1973. The flows were measured on 21 ABSs, and hydrological surveys were performed in parallel. An important novelty was the observation of a change in the flows, made with the help of neutral-buoyancy floats deployed at a depth of 1500 m. Just like in Poligon-70, in the MODE experiment an anticyclonic eddy was discovered in the upper half of the ocean. Its horizontal extent was about 80 km—somewhat smaller than on Poligon-70 (owing to the shorter Rossby radius, namely, $L_R = 50$ km in the region of MODE and $L_R = 65$ km in Poligon-70). The eddy drifted westward with an average speed of about 3 cm/s; its orbital velocity was approximately one and a half times higher than for the anticyclone of Poligon-70. The dynamics of the flows turned out to be substantially nonlinear. According to the estimates made by McWilliams[42] vertical stretching of the flux lines and local change in the vorticity made the main contribution to the balance of the potential vorticity, while the beta effect was relatively small. Calculations of the frequency spectra of oscillations of the water temperature revealed a maximum at a period of about 140 days, which agrees with the estimated size of the MODE eddy and its westward drift speed, given above.

More detailed measurements of synoptic vortices in the open ocean were performed in the Soviet-American experiment POLYMODE in the Sargasso Sea from July 1977 to September 1978. American Lagrangian measurements were performed with the help of neutrally buoyant Sofar floats at depths of 700 and 1300 m in parallel with Soviet Eulerian

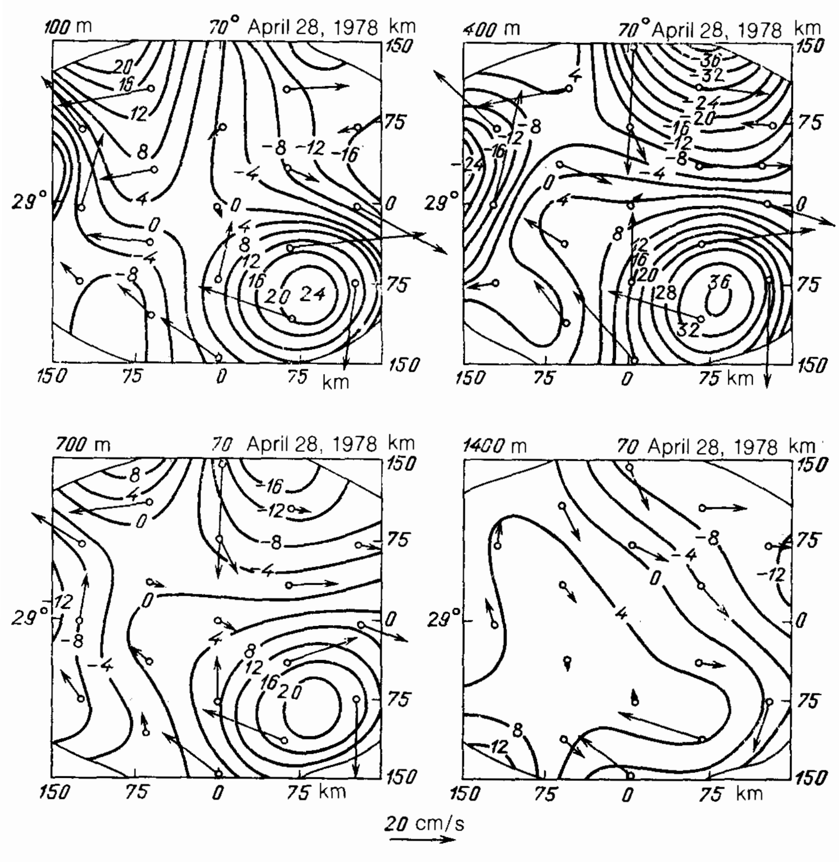

FIG. 10. Velocity vectors and streamlines of synoptic flows at the 100, 400, 700, and 1400 m levels in the POLYMODE region on April 28, 1978.

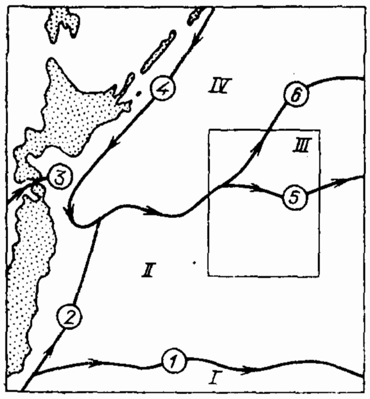

FIG. 11. Megapoligon.

measurements of the velocity field at 19 AFSs with 76 flowmeters (at depths of 100, 400, 700, and 1400 m). Figure 9 shows the frequency spectra of the kinetic energy on the survey area as an average over all AFSs (according to Ref. 43). Aside from the two narrow peaks at periods of 12.4 h (semidiurnal tide) and 24 h (diurnal tide and inertial oscillations) these spectra have a wide maximum at synoptic periods ranging from 30 to 170 days. A total of 13 synoptic eddies, of which six anticyclones had sizes corresponding to a Rossby radius $L_R = 50$ km, were recorded in the survey area over the period of the observations.

The eddies turned out to be closely spaced (complete data of this type were recently published in the atlas of Yu. M. Grachev *et al.*[44]) and in most cases were substantially baroclinic, i.e., they changed appreciably with depth (see, for example, Fig. 10). Synoptic charts of the temperature and salinity, constructed from hydrological data, on the whole agreed quite well with eddies in the velocity field of the flow: regions of elevated temperature and salinity corresponded to the central parts of strong anticyclones while regions with low values corresponded to the central parts of cyclones; this is apparently connected with the vertical motions in synoptic eddies. All eddies move predominantly westward with an average speed ranging from 2 to 7 cm/sec. Calculations showed that the kinetic energy of the eddies in the survey area fluctuated significantly (Fig. 3 and its discussion). An extensive summary of the observational data was published in 1986 in the Soviet-American Atlas POLYMODE.[45]

An observational experiment on an even larger spatial scale was organized by the Institute of Oceanography of the Academy of Sciences of the USSR in the interagency expedition Megapoligon (June–November 1987). The main problem addressed by this expedition was to study the field of synoptic eddies and its evolution over a large area. For this a region with a completely different hydrodynamic environment than in the POLYMODE experiment was selected: an area of about 500×500 km^2 in the Pacific Ocean east of Japan and north of the Kuroshio current and centered at 45°53′ N.L., 154°34′ E.L. near the point of bifurcation of the sub-Arctic flow (Fig. 11).

The main work which, until recently, distinguished Soviet oceanography in general and the Institute of Oceanography of the Academy of Sciences of the USSR in particular was direct measurements of currents. For this about 180 AFSs with 440 flowmeters (these are record high numbers for international oceanography), deployed at depths of 120 and 1200 m and in some of the AFSs at depths of 400 and 4500 m also, were distributed over the Megapoligon survey area. Measurements on the network of AFSs were performed primarily in the period from August 10 to October 13, 1987. In addition, in the period from June 14 to November 2, 1987 six hydrological surveys were performed on the Megapoligon survey area using CTD probes to a depth of 1500 m with distances of 20 miles between the stations, and 46 three-day facsimile maps of the temperature of the ocean surface (TOS) were received by radio from Tokyo.

The field of ocean eddies on the Megapoligon survey area turned out to be substantially different[12] from that in the POLYMODE region. As an example Fig. 12 shows a map of isolines of the stream function and velocity vectors of the flows at a depth of 120 m for October 1, 1987; regions with cyclonic vorticity are marked by dots. Six cyclonic and

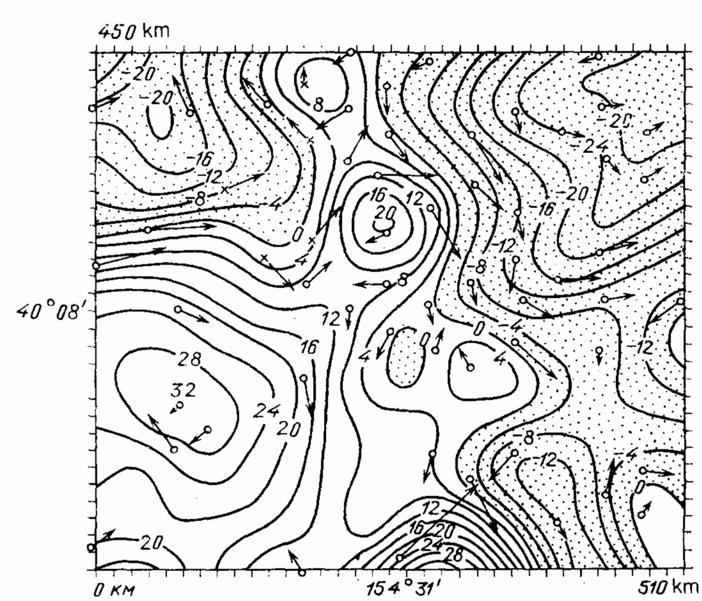

FIG. 12. The velocity field at a depth of 120 m on the Megapoligon survey area on October 1, 1987.

seven anticyclonic eddies can be seen in this map. According to the most detailed measurements performed in the period from August 10 to October 13, 1987 not all of these eddies showed a tendency to move westward. The three largest eddies in Fig. 12—cyclonic northwestern and northeastern and anticyclonic southwestern—are quasistationary. The so-called northern sub-Arctic front, passing between the two named quasistationary cyclonic eddies—northwestern and northeastern—exhibited the main dynamic activity.

The frontal zone between the two eddies of the same sign is essentially a somewhat diffuse zone of the tangential discontinuity of the velocity. It is hydrodynamically unstable (this feature is called the Helmholtz instability), and when it becomes unstable a chain of eddies with opposite sign forms (in Fig. 12—a chain of small anticyclones). Second-order frontal zones form between them; chains of third-order eddies with the same sign form in them; etc. As a result a well-known cascade process whereby vorticity is transferred along the spectrum of scales from large to small scales forms. Of course, only the first cascade of this process—with first- and second-order eddies—can be traced in the Megapoligon network of AFSs.

Over the above-indicated period of measurements on the Megapoligon survey area the chain of anticyclonic second-order eddies seen in Fig. 12 broke down twice (with the formation of a cyclonic bridge, interrupting the northern sub-Arctic front, but restoring the southern sub-Arctic front along its southern periphery, between the cyclonic first-order eddies; the entire flow field weakened in the process) and was restored twice (interrupting the southern sub-Arctic front, but restoring the northern front, with a general intensification of the flows).

It is important to note that the maps of the TOS are in satisfactory agreement with the maps of synoptic flow at a depth of 120 m: regions with cyclonic vorticity and especially cyclonic eddies, as a rule, correspond to low TOS while anticyclonic regions correspond to high TOS. This can be explained by the fact that upwelling, which carries cold deep waters to the surface, occurs in cyclonic eddies (while in anticyclonic eddies, conversely, downwelling occurs). As an example Fig. 13 shows maps of the stream function ψ (according to Ref. 46; the zero point was chosen so that the isoline $\psi = 0$ separates best the cyclonic and anticyclonic regions) and the TOS for October 1, 1987. The correlation coefficient between these maps is equal to 0.72. The linear regression equations have the form

$$\psi = 0{,}5 + 5{,}07(T - 19{,}9), \quad T = 19{,}9 + 0{,}103(\psi - 0{,}5).$$

The good agreement between the anomalies of the TOS and the values of the vorticity $\Delta\psi$ indicates that the other factors involved in the formation of the TOS (i.e., heat and moisture transfer between the ocean and the atmosphere) are weaker.

If this last result is true not only in this region and during this season, for which there is hope, then it could give a scientific basis for employing the data from the Razrezy program (conducted in the last five years) for long-range weather forecasting. Long-range forecasting requires prediction of the TOS, which is in principle possible on oceanic synoptic time scales—weeks and months—according to the following scheme: the initial TOS field is measured by aerocosmic methods; the initial field of synoptic flows in the upper layer of the ocean is reconstructed from this field, for example, by means of regression equations; the synoptic flow field is extrapolated into the future with the help of eddy-resolving models; then the forecasted TOS fields are constructed using regression equations. This scheme can be improved in two ways. First, the simplest improvement is to add a three-dimensional construction of the TOS fields, measured in real time by aerocosmic methods, in the coordinates (x,y,t). The second and profound improvement is to combine the described scheme with long-range weather forecasting taking into account feedback—the action of the atmosphere on the ocean via wind stress as well as heat and moisture transfer.

Another important result of Megapoligon was the discovery of quite strong synoptic flows, at times and in some places reaching 40–50 cm/s, at a depth of 1200 m with significantly larger eddies than in the upper layer of the ocean (in which the meanders of the fronts do not penetrate to large depths, since the T,S curves of the waters separated by the fronts rapidly approach one another as the depth increases). These currents have a tendency to drift westward and exhibit a quite strong (sometimes even rapid) variability in time. In contradistinction to the upper layer the deep circulation often turned out to be cyclonic in the southern half and anticyclonic in the northern half of the Megapoligon survey area. This happened, for example, on September 19, 1987, when the entire Megapoligon area was occupied by a gigantic wave on a westward current with a deep cyclonic trough, penetrating from south to north at the center of Megapoligon, and anticyclonic crests, oriented from north to south, along the edges (Fig. 14). The overall impression is that the deep current, on the average flowing westward, is a compensating

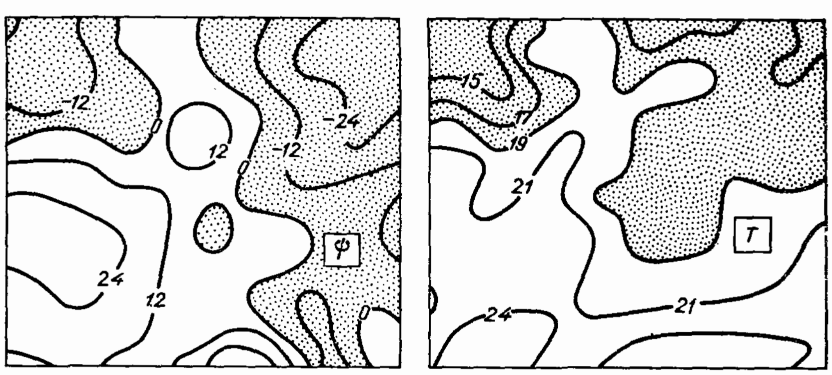

FIG. 13. The correlation between the maps of the stream function ψ and the surface temperature of the ocean T on the Megapoligon survey area in the period from September 29 to October 2, 1987.

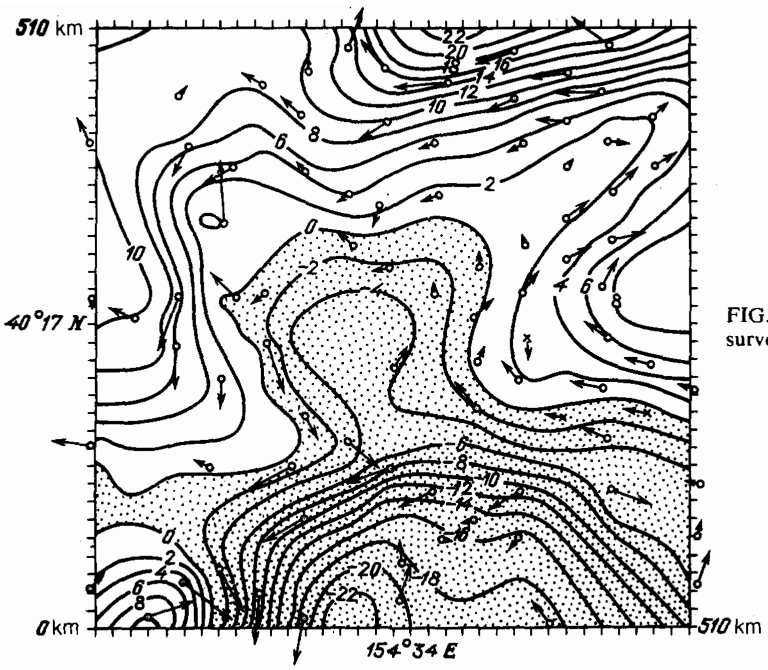

FIG. 14. The velocity field at a depth of 1200 m on the Megapoligon survey area on September 19, 1987.

countercurrent for the total eastward flow in the upper layer. This is apparently a manifestation of the characteristic tendency of ocean currents to compensate locally the water flow rates.

We note that the configuration of the synoptic flows at a depth of 4500 m, measured on a 350×210 km^2 rectangle in the southeastern part of the Megapoligon survey area in the period from September 15 to October 13, 1987, corresponded well to the flows at a depth of 1200 m, and these flows turned out to be strong: up to 20–30 cm/s. In the southern half and the north of the indicated rectangle they were directed westward, and in the strip between them a chain of anticyclonic eddies, drifting slowly westward, was observed (see for example, Fig. 15). The synoptic component of these flows probably consists of Rossby waves, generated by the β effect and, possibly, the bottom relief.

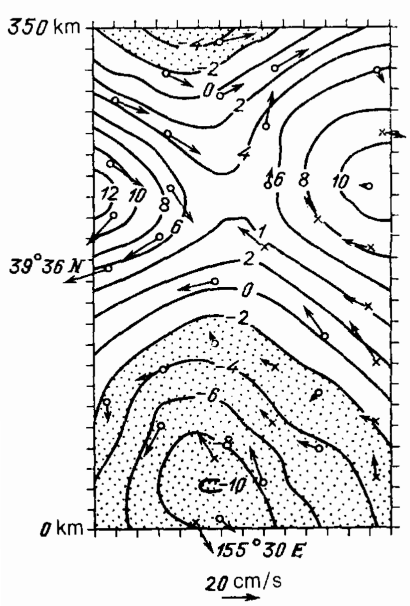

FIG. 15. The velocity field at a depth of 4500 m on the Megapoligon survey area on October 13, 1987.

Observational experiments of the Megapoligon type should definitely be continued.

Synoptic eddies in the ocean are formed as a result of baroclinic and barotropic instabilities of large-scale flows as well as atmospheric actions and the effects of flow over irregularities of the bottom relief. This diversity of mechanisms of generation explains the observed prevalence of synoptic eddies. To discuss the conditions of instability of flows whose stream function ψ satisfies Eq. (4) we shall study their total (specific) energy (which is, of course, an adiabatic invariant):

$$\mathscr{H} = \frac{1}{2H}\int\left[|\nabla\psi|^2+\frac{f_0^2}{N^2}\left(\frac{\partial\psi}{\partial z}\right)^2\right]dx\,dy\,dz+\frac{1}{2}\int k_0^2|\psi|^2dx\,dy, \qquad (14)$$

where $k_0^2=f_0^2/gH$. The first term here corresponds to the kinetic energy K, and the second and third terms correspond to the available (i.e., capable of transforming adiabatically into K) potential energy P (the second term P_1 is the baroclinic term and the third term P_2 is the barotropic term). For flows with horizontal scale L their ratios are $K:P_1:P_2=1:(L/L_R)^2:(L/L_0)^2$, where $L_0=k_0^{-1}$. In the ocean $L_R\sim 50$ km (and $L_0\gg L_R$, so that $P_2\ll P_1$), and for large-scale flows with $L\sim 1000$ km $\overline{P}\sim 400\overline{K}$ is of the order of 7×10^2 J/m^3 according to the empirical estimate made by I. A. Bulis and A. S. Monin,[47] while for synoptic flows with $L\sim L_R$ $P'\sim K'$ is of the order of 20 J/m^3 according to the empirical estimate made in Ref. 48, i.e., the kinetic energy of the synoptic eddies K' is on the average an order of magnitude higher than the value of $\overline{K}$ for large-scale flows, but $K'+P'$ is an order of magnitude lower than $\overline{P}$; this last fact means that the generation of eddies has virtually no effect on the large-scale inclinations of the isentropic surfaces.

With the help of the equations of hydrodynamics it can be proved that in baroclinically unstable disturbances of *zonal* flow $U(y,z)$ the particles of liquid must move along trajectories that are sloping relative to the horizon in the meridional plane $w'/v' \sim (UH/L)/f_0 L$, so that their slope is bounded by the slope of the isentrope $f_0 U/N^2 H$, whence $(L_R/L)^2 \leqslant 1$, i.e.,the scales L of baroclinically unstable disturbances cannot be much less than L_R. J. Pedlosky[49] established that the increment of growth of unstable disturbances decreases as L increases, so that it can be expected that even for developed disturbances $L \sim L_R$. A number of necessary conditions for instabilities can be formulated in terms of a meridional gradient of the potential vorticity of zonal flow $B = \beta - \partial^2 U/\partial y^2 - (\partial/\partial z) \downarrow (f_0^2/N^2) \partial U/\partial z$; 1) either B is a sign alternating or somewhere $(\partial U/\partial z)_{z=-H}$ has the same sign as B, or somewhere the sign of $(\partial U/\partial z)_{z=0}$ is opposite to that of B; 2) either somewhere $UB > 0$ or somewhere $(U \partial U/\partial z)_{z=-H} < 0$, or somewhere $(U \partial U/\partial z)_{z=0} > 0$.

In the two-layer model it is possible to give the necessary and sufficient condition:[49] the values of $U_1 - U_2$ must lie outside the interval $(-FH_1, FH_2)$, where $F = \beta f_0^{-2} g(\rho_2 - \rho_1)\rho_1^{-1}$, and the index 1 corresponds to the upper layer while the index 2 corresponds to the bottom layer. G. M. Zhikharev[50] studied in such a model the stability of the simplest nonzonal flow $U_1 = \text{const}$, $U_2 = 0$ above a wavy bottom relief $H = H_0 \sin(k \cdot x)$ (see also J. Charney and G. Flierl,[51] A. Buzzi *et al.*,[52] and J. Pedlosky[49]). He proved for the examples calculated that with fixed $|k|$ an increase of the shear $|U_1|$ results first in orographic and then baroclinic instability, i.e., the former is a kind of catalyst for the latter.

The effects of flow over irregularities H' of the bottom relief $z = -H + H'$ become comparable to the β effect when $H'/H \sim L/R_0$ (where R_0 is the earth's radius), and the critical value $H' = HL/R_0$ in the ocean is ten times smaller than in the atmosphere, which is why topographic eddies are much more common in the ocean. Because of the smallness of H'/H they satisfy the boundary condition $w \equiv -(f_0^2/N^2)\partial^2\psi/\partial z \partial t = J(\psi, H')$ at $z = -H$. We shall confine ourselves for the time being to barotropic disturbances. For them we have now instead of Eq. (4) (see Sec. 39 of Ref. 4) the law of conservation of the quantity $q = (f + \Delta\psi - k_0^2\psi) H_0^{-1}$, where $H_0 = \zeta + H - H'$ is the total thickness of the ocean ($z = \zeta$ is the disturbed level of the ocean, which we shall neglect in what follows). In linearized form it is expressed by the equation

$$\frac{\partial \Delta\psi}{\partial t} + \beta \frac{\partial \psi}{\partial x} + J(\psi, H') = 0, \tag{15}$$

which shows that the irregularities $H'(x)$ play a role analogous to the β effect. If their horizontal scale $L_h \gg L$, then the bottom is said to be *sloping*, and $\nabla H'$ can be regarded as locally constant. For wave disturbances in this case the frequencies $\omega = (F_x k_y - F_y k_x) k^{-2}$, where $F = \beta y + (f_0 H'/H)$ are obtained. If $L_h \ll L$, then the bottom is said to be *rough*. For a cylindrical relief $H'(y)$ (Ref. 53) the dispersion relation is

$$\omega^2 + \omega\beta k_x k^{-2} - f_0^2 \left(\frac{k_x}{k}\right)^2 \frac{\overline{H'^2}}{H^2} = 0, \tag{16}$$

so that small-scale roughness of the bottom can engender large-scale waves (and this paradox is intensified by the fact that the energies of the large- and small-scale motions here are comparable, so that smoothing of the bottom relief in calculations of large-scale flows can produce significant errors).

For $L_h \propto L$ the bottom is said to be wavy. It is capable of both partially reflecting waves and engendering trapped modes.[54-56] We shall examine the last effect for the example of baroclinic flow past an isolated mountain, following H. Huppert and K. Bryan.[57]

Because the potential vorticity is conserved (for $\beta = 0$ and $N = \text{const}$) under conditions of upwelling of cold waters along the slope $-\partial\rho'/\partial z$ increases and the relative vorticity $\Delta\psi$ decreases, while under conditions of downwelling $\Delta\psi$ increases. As a result, a cold anticyclonic eddy forms above the mountain and a warm cyclonic eddy forms downstream from the mountain. The anticyclonic eddy always remains above the top of the mountain. The cyclonic eddy with small $NH'/U \sim 1$ is carried by the flow downstream (eddies are more intense in this case), while for $NH'/U \sim 10$ it remains "tied" near the anticyclonic eddy (and the eddies are not as strong—this case is apparently typical for the real ocean); examples of a numerical calculation are shown in Fig. 16.

J. Verron[58] made this problem more complicated: he studied a flow that varied periodically with time $U = U_0(1 - \cos \omega t)$. His calculations show that both in the barotropic case (with the potential vorticity $\Delta\psi + (f_0 H'/H)$ and in the baroclinic case with small U an anticyclone and a cyclone form above the mountain. But when U exceeds some critical value (and the period $2\pi/\omega$ is less than the typical advection time L/U_0, where L is the diameter of the mountain), then not only the cyclonic eddy but also the entire cyclone-anticyclone pair can become detached. In the process a chain of pairs of eddies is formed beyond the mountain (according to Verron's calculations the β effect cannot change this picture qualitatively). Such flow past Corner Rice sea mounts possibly explained the looping trajectories of four buoys in the region of the return flow of the Gulf Stream.[59]

Synoptic eddies can also be generated by direct atmospheric actions—wind stress, nonuniformities of the atmospheric pressure, and flows of heat and salt (engendering a "flow of buoyancy"). Empirical data on the space-time spectra of these fields on the scales of synoptic motions have been studied by L. Magaard,[60] J. Willebrand,[61] and in especially great detail by C. Frankignoul and P. Muller[62] (see Sec. 3.3 of Ref. 9 or Sec. 42 of Ref. 4 for the details). These studies showed that of the factors mentioned above the wind stress plays the main role. At moderate latitudes the spectra of the atmospheric actions have maxima at periods of several days and wavelengths of 3–6 thousand kilometers, characteristic of atmospheric synoptic processes, but they contain significant energy both at lower frequencies and smaller spatial scales. At periods exceeding 10–20 days the temporal spectra become weakly frequency dependent, and at wavelengths less 3 km the spatial spectra approach isotropic spectra. The empirical model $F_k = F_0 k^2 S_k$, $F_0 = 10^4 H^2 (M^4 \Gamma II)^{-1}$ where S_k is the spatial spectrum normalized to unity and is proportional to k^{-3} at wavelengths less than 5 km, is applicable for the space-time spectrum of a wind-stress eddy at low frequencies. Here the westward motions of the atmospheric disturbances, capable of exciting in a reso-

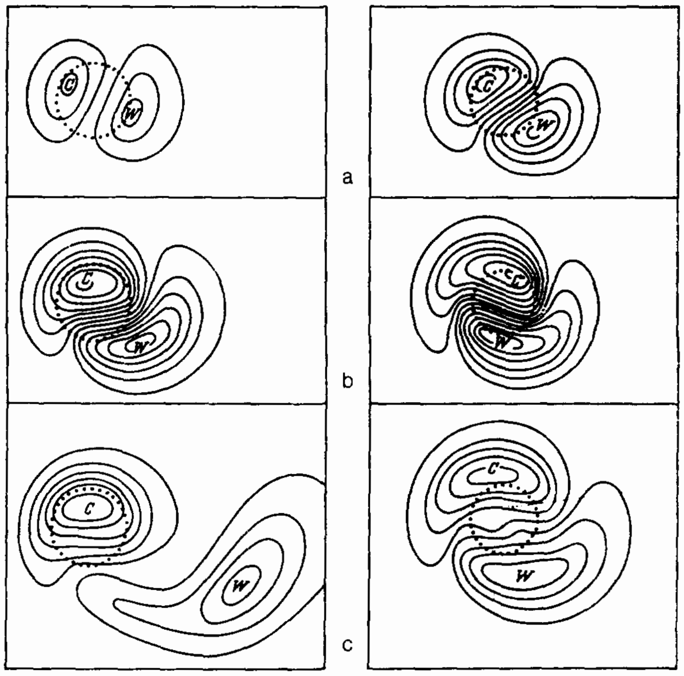

FIG. 16. Distribution of isopeaks at a depth of 3720 m with time intervals from the moment of development of the flow of 4.6 days (a), 9.3 days (b), and 23.1 days (c).[50]

nant fashion Rossby-Blinova waves in an ocean with a flat bottom, are also taken into account. The corresponding fluxes of energy (in the wavelength range from 4 to 50 km) into the barotropic mode of the total and kinetic energies turned out to be equal to 2.9×10^{-4} and 2.85×10^{-4} W/m^2, i.e., almost the entire flux goes into increasing the kinetic energy of waves with long wavelengths. The analogous fluxes into the baroclinic mode are equal to 1.5×10^{-4} and 0.5×10^{-4} W/m^2, i.e., the flux goes primarily into increasing the available potential energy. The total flux of 0.44×10^{-3} W/m^2 is comparable to the space-averaged estimate 10^{-3} W/m^2 of the flux from the baroclinic instability,[63] but in the zones of stream flows that latter is much larger. Thus direct atmospheric action can engender barotropic synoptic disturbances in the open ocean. If the ocean bottom is uneven, then resonance generation is also possible due to atmospheric disturbances moving eastward.

6. EDDY-RESOLVING MODELS

Mathematical modeling of the ocean circulation consists of calculating the basic hydrodynamic fields (flow velocities, surface level, temperature, salinity and density of the water) for given external actions (primarily atmospheric action).

This obvious formulation is presented here because there are publications (summarized in Ref. 7 and in publications preceding it[64]), in which a different, so-called diagnostic, problem is proposed—calculation of the velocity field of large-scale flows based on given water temperature and salinity fields and the wind action. However, within the framework of hydrodynamics, the density (temperature and salinity) fields and the external action fields cannot be specified independently of one another—the former are functionals of the latter. In Refs. 7 and 64 diagnostic calculations were performed using an arbitrarily simplified equation (the dependences of the density on the pressure, lateral mixing, etc., were ignored). In many regions their results contradicted the measurements (for example, the computed counterflow underneath the Gulf Stream is not observed in nature).

Returning to hydrodynamics, we mention mathematical models of the large-scale circulation of the atmosphere in which lateral mixing engendered by synoptic eddies was "parametrized" as an effect of "horizontal" turbulent viscosity with a large positive constant coefficient $\mathscr{K}_h \sim 10^7 - 10^8$ cm^2/s (brief reviews of such models are given in, for example, Refs. 4 and 21). Among the most detailed models of this type we mention the 12-level model of Ref. 65, employed in Ref. 66 to calculate the state of the ocean with fixed atmospheric actions with a seasonal trend (on a grid with a horizontal step of 500 km). We note that according to this calculation the temperature in the deep layers of the ocean did not reach a steady value even after 1200 model years (but rather it continued to increase at a rate of about 0.1 °C/100 yr, which corresponds to a heat flux from the atmosphere of less than 0.25% of the solar constant): The deep ocean adjusts to atmospheric actions very slowly.

However specifying positive values of $\mathscr{K}_h$ precludes any action of "negative viscosity," i.e., the inherent capability of an ensemble of synoptic eddies to transport a statistically averaged momentum from regions of space where this density is low to regions where it is high, and thereby form the observed narrowness of the main oceanic currents (for example, the Gulf Stream is only 70-90 km wide).

Negative viscosity in ensembles of synoptic eddies is an important phenomenon of nature. Apparently this phenomenon explains the differential rotation in the earth's atmosphere (subtropical currents), on the surfaces of large planets, and on the sun (equatorial acceleration) with formation of toroidal magnetic fields from poloidal fields, i.e., half the cycle of a hydromagnetic dynamo; all this could be a universal property of spherical, rotating, electrically-conducting, gaseous bodies.[67]

Negative viscosity in the ocean was discovered by F. Webster,[68] V. Starr,[69] R. V. Ozmidov *et al.*,[70] and A. S. Monin and D. G. Seidov.[71] Its "parametrization" for the ocean was not yet developed (while for zonal models of the atmosphere, for example, G. Williams and D. Davis[72] proposed a formula), but it may be possible to take it into account completely by describing individually all the synoptic eddies engendering it. Such an *eddy-resolving* model of ocean circulation must be constructed on a spatial grid with a horizontal step size not greater than the Rossby radius of deformation L_R, i.e., not more than several tens of kilometers.

The first eddy-resolving model was constructed in 1975 by W. Holland and L. Lin.[73] This was a two-layer model with the complete equations on a grid consisting of 51×51 points in a 1000×1000 km^2 ocean of constant depth with wind excitation engendering an anticyclonic gyre. Barotropic synoptic eddies appeared in its northern section as well as in the return flow in the eastern and southern regions. Sometimes, baroclinic synoptic eddies also appeared in the return flow. The quasigeostrophic two-layer model developed by W. Holland gave analogous results.[74]

The numerical experiments performed by P. Rhines with single-layer[25] and two-layer[76] eddy-resolving models played an important role in understanding the statistical dynamics of synoptic flows described by Eq. (4). These calculations establish that, on the average, synoptic eddies evolve in time as follows:

1) they grow in size;

2) they acquire a tendency to drift westward and become anisotropic, approaching zonal flows; and,

3) they become barotropic, i.e., they become vertically homogeneous.

The first two of these characteristics can be understood with the help of the simplest barotropic model (with viscosity ν). In this model the total kinetic energy $E=(1/2)\langle|\nabla\psi|^2\rangle$ degenerates according to the law $\partial E/\partial t=-2\nu\Omega$, where $\Omega=(1/2)\langle(\Delta\psi)^2\rangle$ is the *enstrophy* (1/2 the total squared vorticity). For small ν the quantity E will be approximately constant, and the energy spectrum in the energy-carrying interval of wavelengths k will have the self-similar form $E^{3/2}tf(E^{1/2}kt)$ (G. Batchelor[77]). Then the equation $\partial k_*^{-1}/\partial t=cU$ is obtained for the wave number k_* averaged over the spectrum; here $(1/2)U^2=E$ and c is a positive number, so that the average scale of the eddies $L=2\pi k_*^{-1}$ increases with time.

Equation (4), owing to the term $J(\psi,f)=\beta\partial\psi/\partial x$ (the β effect), describes not only eddies (carrying water with them), but also Rossby-Blinova waves (traveling along the water) engendered by the β effect. Their relative role $J(\psi,f):J(\psi,\Delta\psi)$ is equal to c_0/U, where $c_0=\beta/(2k^2)$ is the phase velocity of the waves, so that eddies predominate for $k>k_B=(\beta/2U)^{1/2}$ and waves predominate for $k<k_\beta$. In Ref. 75 a field of closely spaced eddies with a narrow spectral peak for $k_0>k_\beta$ was chosen for the starting field, and the scale of the eddies L_* increased with time in the manner indicated above with the coefficient $c\approx 3\times 10^{-2}$, but after the scale $L_\beta=2\pi k_\beta^{-1}$ was reached this growth continued slowly with the coefficient $c\approx 6\times 10^{-3}$.

Waves grow more slowly, since their interactions require that three waves add in space and that the wave frequencies and vector be in resonance, and such interactions tend to transfer energy to the wave whose frequency $\omega=-\beta k_x k^{-2}$ is lowest and whose direction of propagation k is closest to the zonal direction (anisotropization, whose limit is striped zonal circulation, like on large planets). The transformation of eddies into waves (primarily the appearance of a tendency to drift westward) can be seen clearly in Fig. 17 (taken from Ref. 75).

In the baroclinic model in Ref. 4 the two terms in the relative vorticity $\mathscr{L}\psi$ must be compared. For $k>k_R=2\pi L_R^{-1}$ the term $\Delta\psi$ predominates and vertical interactions between different layers of the liquid play a small role, so that the flows in these layers evolve approximately independently of one another (baroclinic eddies). Conversely, for $k<k_R$ interaction along the vertical between different layers predominates, and the layers evolve as a single layer (barotropic eddies). In the two-layer model[76] for $k_0>k_R$ as k_* increased to the value k_R barotropization was complete and occurred very rapidly (see Sec. 3.5.7 of Ref. 9 for a more detailed discussion). In the ocean, as a rule, $L_\beta>L_R$, so that evolution proceeds in the sequence baroclinic eddies → barotropic eddies → barotropic waves (and linear baroclinic waves can arise primarily only as a result of external ac-

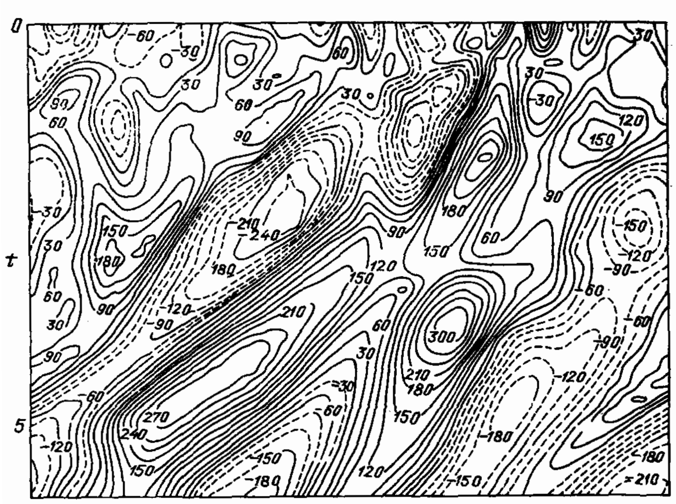

FIG. 17. The evolution of the stream function field in time-longitude coordinates according to Rhines.[75]

tions—due to the atmosphere, the bottom, and the shores).

Multilayer eddy-resolving models were also constructed immediately. In the USSR the first eddy-resolving model was D. G. Seidov's five-level model[78] of the circulation in a basin with the dimensions $960\times1440\times5$ km^3. The flows were divided into deep-averaged and quasigeostrophic shear flows, the zonal wind action generated near the middle latitude an eastward current, and a vertical heat flux proportional to the temperature difference between the water and the air was given on the surface of the basin. The model was integrated on a spatial grid with $25\times37\times5$ nodes over a time period of ten years with a time step of 6 h (other variants were also calculated).

The numerical experiments with this model led to the following conclusions:

1) nonlinear (inertial) effects were important for synoptic eddies (in contradistinction to large-scale gyres);

2) eddies engendered "tunneling" transfer of heat through zonal currents as well as concentration of heat in the flows at the western boundary;

3) the energy transformations turned out to be sharply spatially nonuniform, and in the zones of stream flows negative viscosity played an important role—the volume-averaged energy cycle had the form $\bar K\to P\to K'\to\bar K$ (in addition, feedback was weak only when averaged over the volume, and in the zones of stream flows it played a decisive role);

4) the energy cycle in the system full flows—shear flows had the form $K'\to(P,\bar K)$, and in addition significantly more energy was transferred to P and $\bar K$ from K' (i.e., owing to barotropization) than from external sources; and,

5) relaxational oscillations with periods of accumulation and shedding of energy, qualitatively similar to those actually observed (Fig. 3), arose in the circulation.

D. G. Seidov, A. D. Marushkevich, and D. A. Nechaev[79] soon constructed the first eddy-resolving model of the entire ocean with real shoreline contours and bottom relief—of the North Atlantic in the range 13–61° N.L. The model contained seven working levels 0, 200, 500, 800, 1200, 2000, and 3000 m and a horizontal grid of $40\times40'$, and it was integrated using time steps of 12 h over a period of 5 yr. The calculations demonstrated active eddy formation in the zone of the Gulf Stream and the Labrador Current as well as accompanying current flow over the mid-Atlantic ridge. The eddies intensified the Gulf Stream by a factor of 1.5–2 and the Labrador Current by a factor of three, and they maintained in these regions high horizontal temperature gradients. A scheme for realizing this experiment for eddy-resolving modeling of the entire ocean was proposed in Ref. 4. However this work was delayed at the Institute of Oceanography of the Academy of Sciences of the USSR.

The first eddy-resolving global model of the ocean (without the Arctic basin) was constructed in 1988 by A. Semtner and R. Chervin.[16] In this model an even more detailed, than in Ref. 79, spatial grid is employed: 20 levels along the vertical (of these ten are in the upper 710 m) and a 30' step along the horizontal direction were employed. Integration (on a Cray X-MP/48 computer) of the equations of motion and the heat and salt budgets was performed over a period of 20 yr (and required 250 h of machine time) with average yearly wind forcing. During the last ten model years the model was in a statistically steady-state regime (during the last two model years, in order to intensify the synoptic processes generated by the model the harmonic dissipative operators $\mathscr{K}_h\Delta$ were replaced by the biharmonic operators $\mathscr{K}_h L^2\Delta\Delta$). The computed hydrophysical fields agreed with observational data. We note first the nonstationary western boundary flows, during the meandering of which warm and cold rings were engendered. Aside from the Gulf Stream and the Kuoroshio and Oyashio currents, such eddies appeared as a result of the development of instability and other flows, such as the east-Australian, Brazilian, and Falkland currents; eddy activity was also found in some frontal zones of the ACPC.

The most surprising result was the "Indian Ocean express"—the flow of warm thermohaline waters from the tropics of the Pacific Ocean through the Indian Ocean and then into the Atlantic around the southern tip of Africa (with the oppositely directed flow of cold deep abyssal waters from the North Atlantic, already suspected a long time ago by V. N. Stepanov at the Institute of Oceanography of the Academy of Sciences of the USSR and capable of explaining the significant difference in the concentrations of biogenic elements in the three oceans); see the schematic summary of the corresponding factual data in Fig. 18.

The authors of the model[16] feel that an eddy-resolving model of the ocean with 40 working levels and a horizontal

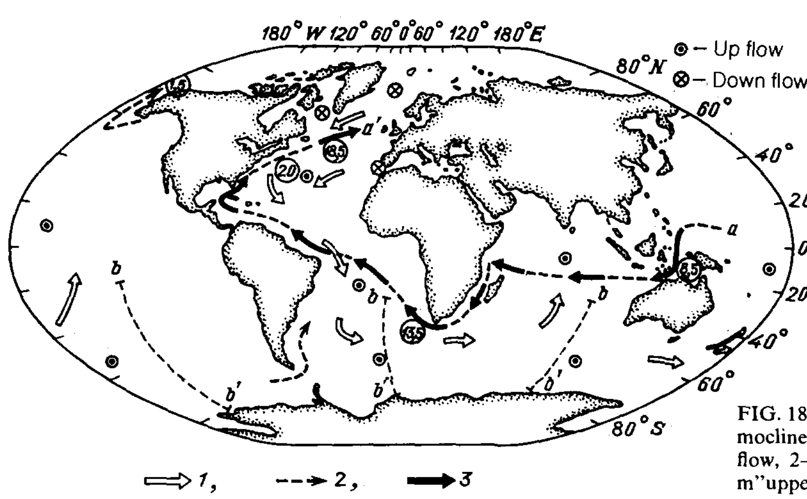

FIG. 18. Diagram of the interocean exchange of deep waters and thermocline waters according to Gordon (see Ref. 16). 1—deep water flow, 2—"cold" water transfer into the Atlantic Ocean, 3—"warm" upper layer flow.

step of 7.5′ can be realistically constructed by 1993; in addition, the calculation over a decade will require not more than 500 h of computer time. Compared with Ref. 16 the book of Ref. 7, which was published at the same time, is clearly late.

7. HAMILTONIAN FORMALISM

Equation (4) for the stream function ψ of synoptic flows in the adiabatic case $\Phi \equiv 0$ can be put into a Hamiltonian form, so that all the results of the general theory of Hamiltonian systems can be extended to it also (V. E. Zakharov and E. A. Kuznetsov[80] and A. Veĭnsteĭn[81]). Namely, denoting by $\Omega = \mathscr{L}\psi$ the relative potential vorticity (for barotropic flows $\Omega = \Delta\psi - k_0^2\psi$, where $k_0^2 = f_0^2/gH$), Eq. (4) can be written in the form $\partial\Omega/\partial t = \{\Omega, \mathscr{H}\}$, where $\mathscr{H}$ is the Hamiltonian, and the braces are the so-called Poisson brackets, which according to Refs. 80 and 81 are defined in this case for any two functions $F[\Omega]$ and $G[\Omega]$ by the formula

$$\{F, G\} = \int (\Omega + \beta y)\, J\left(\frac{\delta F}{\delta\Omega}, \frac{\delta G}{\delta\Omega}\right) dx\, dy\, dz. \tag{17}$$

for $\beta = 0$ the bracket $\{F,G\}_0$ with a variable coefficient Ω, specifying the Hamiltonian structure of the two-dimensional hydrodynamics of an incompressible fluid (in mathematics it is known as the Lie bracket for the group of area-preserving diffeomorphisms of the plane) is obtained, and the bracket $\{F,G\}_1 = \{F,G\} - \{F,G\}_0$ is the well-known Gardner bracket from the theory of integrable systems. In order to apply the general theory the so-called normal canonical variables, which "diagonalize" the Poisson bracket, must be introduced into the Hamiltonian system, but there is no general recipe for doing this.

For Eq. (4) this problem was solved by V. E. Zakharov, A. S. Monin, and L. I. Piterbarg (see Refs. 13-15) with the help of the functional transformation $\Omega(x,y,z) = \eta[x,w(x,y,z),z]$, where $w = y + \beta^{-1}\Omega$. Equation (4) is put into the form $\partial\eta/\partial t = \beta(\partial/\partial x)\delta\mathscr{H}/\delta\eta$, and in the barotropic case, to which we shall confine ourselves here in order to simplify the presentation, the normal canonical variables are obtained in the form $\alpha_{\mathbf{k}} = (-2\beta k_x)^{1/2}\eta_{\mathbf{k}}$, where $\eta_{\mathbf{k}}$ are the Fourier coefficients of the function $\eta(x,y)$. The standard Hamiltonian equations $\partial a_{\mathbf{k}}/\partial t = -i\delta\mathscr{H}/\delta a_{\mathbf{k}}^*$ are already obtained in these variables. Expanding $\mathscr{H}$ in a functional power series in a_k and a_k^* we obtain the frequencies $\omega_k = -\beta k_x(k^2 + k_0^2)^{-1}$ as coefficients in the quadratic term (it turns out that three-wave resonance interactions are possible), three-wave interaction coefficients are obtained in the cubic terms, etc.

In the approximation of weak nonlinearity (when the small parameter ε is introduced in the nonlinear term in Eq. (4), the stream function is sought in the form $\varepsilon\psi_1 + \varepsilon^2\psi_2 + \ldots$, and the slow time $T = \varepsilon^2 t$ is introduced) it is sufficient to truncate the analysis at the cubic Hamiltonian, and the following kinetic equation can be derived for the spatial spectral energy density F_k, defined by the relation $\omega_{\mathbf{k}}\langle a_{\mathbf{k}} a_{\mathbf{k}_1}^*\rangle = F_{\mathbf{k}}\delta_{\mathbf{k}-\mathbf{k}_1}$:

$$\frac{\partial F_{\mathbf{k}}}{\partial T} = 8\pi \int (D_{\mathbf{k}_1\mathbf{k}_2}F_{\mathbf{k}_1}F_{\mathbf{k}_2} + D_{\mathbf{k}\mathbf{k}_1}F_{\mathbf{k}}F_{\mathbf{k}_1} + D_{\mathbf{k}\mathbf{k}_2}F_{\mathbf{k}}F_{\mathbf{k}_2}) \times (k^2 + k_0^2)^{-1}(k_1^2 + k_0^2)^{-1}(k_2^1 + k_0^2)^{-1}\delta_{\mathbf{k}+\mathbf{k}_1+\mathbf{k}_2}\delta_{\sigma_{\mathbf{k}}+\sigma_{\mathbf{k}_1}+\sigma_{\mathbf{k}_2}}d\mathbf{k}_1 d\mathbf{k}_2, \tag{18}$$

where $D_{\mathbf{k}_1\mathbf{k}_2} = (1/2)(k_1^2 - k_2^2)(k_{1x}k_{2y} - k_{1y}k_{2x})$ (this equation was derived by making an expansion in terms of ε by K. Kenyon for $k_0 = 0$,[82] M. Longuet-Higgins and A. Gill for $k_0 \neq 0$,[83] and in greater detail by G.M. Reznik;[84] see also the paper by G. M. Reznik and T. E. Soomere,[85] and Ref. 15 for a Hamiltonian derivation).

Equation (18), like the exact equation, conserves the total energy and the potential enstrophy. The latter is equivalent to the conservation of the zonal momentum $\int k_x F_{\mathbf{k}}\sigma_{\mathbf{k}}^{-1}d\mathbf{k}$. The meridional momentum $\int k_y F_{\mathbf{k}}\sigma_{\mathbf{k}}^{-1}d\mathbf{k}$ is also conserved. The rate of change of the total entropy $\int \ln F_{\mathbf{k}}\, d\mathbf{k}$ is equal to some weighted integral of the square of the quantity $A = \sigma_{\mathbf{k}}F_{\mathbf{k}}^{-1} + \sigma_{\mathbf{k}_1}F_{\mathbf{k}_1}^{-1} + \sigma_{\mathbf{k}_2}F_{\mathbf{k}_2}^{-1}$. For this reason the thermodynamically equilibrium spectra are solutions of the equation $A = 0$ on the "resonance line" $k + k_1 + k_2 = \sigma_{\mathbf{k}} + \sigma_{\mathbf{k}_1} + \sigma_{\mathbf{k}_2} = 0$. The only differentiable solution is the isotropic spectrum $(a + bk^2)^{-1}$, where a and b are constants ("temperatures"), like in the case of two-dimensional turbulence.

Unlike two-dimensional turbulence, however, singular spectra of arbitrary zonal flows $\delta(k_x)\varphi(k_y)$, as well as their sums with the above-indicated isotropic spectrum are also solutions. True, for arbitrary initial data they are, generally speaking, unattainable, since on the k_y axis the spectrum F_k does not change with time at all. But the numerical experiments of Refs. 84 and 85 showed that arbitrary initial spectra have a tendency to evolve into one of the above-indicated thermodynamically equilibrium spectra.

In the process the energy is distributed anisotropically—almost all of the energy is concentrated near the k_y axis, i.e., in the zonal flow (the phenomenon of negative viscosity, created by the nonlinearity and the beta effect), while the remaining energy and almost all of the entropy are distributed over the region $|k_x| > \delta > 0$ of the wave space uniformly over all orientations of the wave vectors in accordance with the spectrum $F_{\mathbf{k}} = (a + bk^2)^{-1}$ (isotropization of the entropy). These arguments explain the results of numerical experiments, presented in Sec. 6, with eddy-resolving models. The circulations on all four large planets, so clearly represented on the pictures obtained in the superb Voyager observational experiments, can apparently serve as natural analogs.

8. ROSSBY SOLITONS

The dispersion present in the wave solutions ψ of the equation of transport of the potential vorticity (4) and described by the nonlinear terms $\partial\mathscr{L}\psi/\partial t + \beta\partial\psi/\partial x$ can compensate the nonlinearity $J(2\psi, \mathscr{L}\psi)$. As a result there can exist steady-state solutions which evolve only by means of transfer of the field ψ without a change of form and with a constant velocity, say with the velocity c in the direction x, so that $\psi = \psi(x - ct, y, z)$. Therefore they satisfy the equation $J(\psi + cy, q) = 0$, which has the general solution $q = F(\psi + cy)$, where F is an arbitrary function.

The boundary condition on the free surface, replaced by its equilibrium level $z = 0$, should reduce to the fact that on it $\partial\psi/\partial z + \psi N^2/g$ must be an arbitrary function $F_0(\psi + cy)$, and in the "solid cover" approximation this refers only to $\partial\psi/\partial z$; analogously, the boundary condition at the bottom, which should be cylindrical here, i.e., it is given by the equation $z = -H + H'(y)$, and which is replaced by its average level $z = -H$, should reduce to the fact that there $\partial\psi/\partial z + H'N^2/f$ must be an arbitrary function $F_H(\psi + cy)$, and in the case of a flat bottom this refers only to $\partial\psi/\partial z$.

The nonlinearity $J(\psi,q)$ decomposes into a "scalar" nonlinearity $J(\psi,\mathscr{L}\psi - \Delta\psi)$ and a "vector" nonlinearity $J(\psi,\Delta\psi)$—in the terminology of M. V. Nezlin; see Nezlin's review Ref. 86 and the works cited there, especially those of Nezlin's group. In the barotropic model with a free surface $\mathscr{L} - \Delta = -k_0^2 = -f^2/gH$, and the "scalar" nonlinearity has the form $-(\psi\partial\psi/\partial x)\times\partial k_0^2/\partial y$, which is the same as in the well-known Korteweig-de Vries equation (in the "solid cover" approximation it vanishes; in the baroclinic model H must be replaced by the "equivalent depth" $g^{-1}(NH/m\pi)^2$, where m is the number of the baroclinic mode).

As in the Korteweig-de Vries case, on "shallow water" this nonlinearity engenders steady-state solitary waves—"scalar" solitons of *upwelling* with $0 < \zeta \ll H$, in our case anticyclonic; see the papers by L. Redecopp,[87] D. Anderson and P. Killworth,[88] J. Charney and G. Flierle,[51] and T. Matsuura and T. Yamagata,[91] G. Williams and T. Yamagata,[92] G. Williams,[93] and others. Quantitatively somewhat different "scalar solitons"—with fluid trapped in their central parts (owing to which their amplitude is not related with the diameter) and, unlike the preceding solitons, with a possible relative upwelling $\zeta(H+\zeta)^{-1}$ that is not small—were obtained by G. G. Sutyrin and I. G. Yushina;[94] in Ref. 86 they are regarded as a more general case, but in our opinion these are no longer solitons (solitary waves traveling along the water), but rather solitary eddies carrying "their own" water.

They are all anticyclonic, because with a different sign the "scalar" nonlinearity cannot compensate the dispersion. Their reality is confirmed by the theoretical proof of their stability in the "beta plane"[95] and the fact that they have been reproduced in laboratory experiments in a layer of shallow water in a rotating paraboloid ($z \approx pr^2, p \approx \Omega^2/2g$) by M. V. Nezlin's group[86] (with quite shallow water and therefore short viscous decay time of the vortices $\nu^{-1}H^2$) and by the group directed by V.I. Petviashvili[96] at the Abastumani Observatory (in Nezlin's opinion,[86] with a paraboloid that is too flat).

In Ref. 86 both small and large paraboloids were employed. In the case of the small paraboloid the diameter $D = 28$ cm, the rotational period $2\pi/\Omega = 0.58$ s, the thickness of the layer of liquid $H = 0.3$–1.2 cm, and the dispersion spreading time of a circular packet of Rossby waves $\tau \approx 8(\beta L_R)^{-1} \approx 7.6$ s. For the large paraboloid $D = 70$ cm, $2\pi/\Omega = 0.84$ s, $H = 1$–5 cm, and $\tau \approx 6.6$ s. The eddies were generated by switching on a "pumping disk" for a short time and they drifted in a direction opposite to the flow; the anticyclones with diameters of the order of $2.5L_R$ formed as attractors and were observed for a much longer time τ (up to $\nu^{-1}H^2$), and with $\zeta(H+\zeta)^{-1} \gtrsim 0.15$, they transported "their own" water. Their collisions were inelastic. Cyclones (in the large paraboloid) were formed with difficulty and decayed over a time τ. All this appears to confirm our opinion that here solitary Rossby eddies are formed rather than solitons.

Experiments on the generation of eddies in a zonal flow with shear, created by differential rotations of two zones of the bottom of the paraboloid, are also described in Ref. 86. In the case of a sharp shear—anticylonic or cyclonic—chains of steady eddies—anticyclones or cyclones (Helmholtz instability)—were produced equally successfully. But in the case of a smooth shear the beta effect is also manifested, and only anticyclones could form from large vortices of size $L > L_R$; in the case of an incoming shear a solitary "autosoliton" with a diameter of about $3.5L_R$ and an upwelling $\zeta \approx H$, modeling the Great Red Spot (GRS) of Jupiter, as proposed by G. S. Golitsyn[97]; formed

According to astronomical data the GRS, which has now been observed for 300 yr, is an anticyclone with a characteristic rotation period of about one week; it has a size of 13×26 thousand kilometers, it is located near 22° S.L. in an approximately isothermal, extremely cold layer of clouds with an effective thickness $H \sim 20$ km, and it is drifting westward with a speed of about 3 m/s (according to Ref. 86 the first baroclinic mode of "scalar" Rossby eddies on a zonal flow with anticyclonic shear corresponds satisfactorily to these parameters). The anticyclonic white ovals of Jupiter in the zone near 34° S.L. can be explained analogously, while the brown ovals ("barges") at 14° N.L. on Jupiter are eastward drifting cyclones in a zone with a sharp cyclonic shear. The importance of all these arguments was strengthened after the discovery of eddies by the Voyager space probes on other large planets also, including the analog of the GRS on Neptune.

We shall now discuss solitons generated by the "vector" nonlinearity (see the review by A. L. Berestov and A. S. Monin,[98] Sec. 2.3 of Ref. 9, and Sec. 40 of Ref. 4). For simplicity we shall first study the barotropic model in the "solid cover" approximation, so that for the steady-state solution Eq. (4) will have the form $J(\psi + cy, \Delta\psi + \beta y) = 0$ (however, a free surface and an inclined bottom can be retained, replacing β by $\beta + (f_0^2 c/gH) + (f_0/H)\partial H'/\partial y$). Here it is convenient to transform to polar coordinates, setting $x = r\cos\theta$, $y = r\sin\theta$. We shall confine our attention to solutions of the form $\psi = \Psi(r)\sin\theta$. Then our equation will assume the form

$$\xi\frac{\partial\eta}{\partial\xi} - \eta = 0, \quad \xi = \Psi(r) + cr, \tag{19}$$

$$\eta = \left(\frac{\partial^2}{\partial r^2} + \frac{1}{r}\frac{\partial}{\partial z} - \frac{1}{r^2}\right)\Psi + \beta r. \tag{20}$$

The solution can be constructed following the example with $\beta = 0$ given in Sec. 165 of H. Lamb's book:[99] $c^{-2}\Psi = 2J_1(kr)/kJ_1(kr) - r$ for $r < a$, and $c^{-2}\Psi = -a^2r^{-1}$ for $r > a$, where $J_1(ka) = 0$ and c is arbitrary; here Ψ, $\partial\Psi/\partial r$ and $\partial^2\Psi/\partial r^2$ are continuous at $r = a$. The extension to the case $\beta \neq 0$ but $c = 0$ was obtained by M. Stern,[100] who set $\eta = -k^2\xi$ for $\xi < 0$, whence $\Psi = AJ_1(kr) - \beta k^{-2}r$, and a is chosen so that $\Psi(a) = 0$, after which k is chosen so that $\Psi'(a) = 0$. For this ka must be a zero of the function $J_2(z)$, and the condition $\Psi < 0$ for $r < a$, which is necessary here in order that η depend only on ξ, and not on ξ and r (Stern did not point this out), is satisfied only for the first of these zeroes. For $r > a$ Stern set $\Psi = 0$, which for $r = a$ ensured that Ψ and $\partial\Psi/\partial r$ but not $\partial^2\Psi/\partial r^2$ are continuous (discontinuity of the vorticity).

The extension to the case $\beta \neq 0$ and $c \neq 0$, i.e., a drifting Rossby soliton, was obtained by V. D. Larichev and G. M. Reznik.[101] To demonstrate their solution we shall set $\eta = -k^2\xi$ for $\xi < 0$ and $\eta = l^2\xi$ for $\xi > 0$. It turns out that in order for Ψ to decay exponentially as $r \to \infty$ it is necessary that $l = (\beta/c)^{1/2}$, and in addition it is necessary that $\beta/c > 0$, for which c must lie outside the interval

$$\left[-\left(\beta + \frac{f_0}{H}\frac{\partial H'}{\partial y}\right)\frac{gH}{f_0^2}, 0\right]$$

(for $c > 0$ the soliton drifts eastward; the velocities of periodic Rossby waves lie in the interval itself). The solutions of Eq. (20) are cylindrical functions, and the integration constants are chosen so that the functions Ψ and $\partial\Psi/\partial r$ are continuous at $r = a$; the latter gives the dispersion relation $c = c(k,a)$ in the form $-(ka)^{-1}J_2(ka)/J_1(ka) = (la)^{-1}K_2(ka)/K_1(ka)$ (in addition, in order that the conditions $\xi < 0$ and $r < 0$ coincide the quantity ka must fall between the first zero and the second minimum of the function $(kr)^{-1}J_1(kr)$; see, for example, Ref. 98). We note that here $\partial^2\Psi/\partial r^2$ is continuous at $r = a$, but $\partial^3\Psi/\partial r^3$ is discontinuous. Because of the factor $\sin\theta$ the soliton is, of course, a dipole.

The stability of the shape of solitons of the indicated type ("modons") was proved analytically by V. A. Gordin and V. I. Petviashvili.[102] The solitons were obtained in laboratory experiments by R. Davis and A. Acrivos,[103] as well as in Refs. 86 and 96. In Ref. 86 they were obtained (though they were not sufficiently long-lived) only on the deepest water ($H \gtrsim 4$ cm) in the large paraboloid—the pumping disk generated a cyclonic disturbance. It decayed into two cyclones, each of which formed of itself an anticyclonic neighbor, and the dipole with the external cyclone drifted westward while the cyclone with an external anticyclone drifted eastward. These dipoles carried "their own" water, i.e., they were more like eddies than waves (i.e., in them the "vector" nonlinearity was stronger than the beta effect).

The interactions of dipoles were studied in the numerical experiments of V. D. Larichev and G. M. Reznik[104] and M. Makino, T. Kamimura, and T. Taniuti[105] (in the example shown in Fig. 19 the large soliton overtakes the small soliton). In Ref. 105 it was established also that when the axis of the dipole is initially tilted with respect to the x axis the trajectory of the dipole oscillates in a wave-like fashion around this axis, and the intensities of the eddy pair oscillate in an alternating fashion.

In Refs. 106 and 107 it is shown that the soliton of Larichev and Reznik $\Psi_1(r) = M_1 J_0(kr) - M_2$ for $r < a$ and $k_0(lr)$ for $r > a$ with definite values of the constants M_1 and M_2 can be added to the stream function $\psi = \Psi(r)\sin\theta$ (but in so doing a discontinuity appears in $\partial^2\psi/\partial r^2$). A. L. Berestov[108] pointed out a three-zone soliton with different $\Psi(r)$ with $r < a$, $a < r < b$, and $r > b$ and with continuous vorticity $\partial^2\psi/\partial r^2$; here a function $\Psi_1(r)$ can also be added to ψ.

In Ref. 107 a family of dipole solitons in a two-layer ocean is constructed. In Ref. 108 a three-dimensional soliton is constructed; in spherical coordinates $x = r\sin\theta\cos\lambda$, $y = r\sin\theta\sin\lambda$, $z = f_0 N^{-2} r\cos\theta$ with $\psi = \Psi(r,\theta)\sin\lambda$ the equation for the potential vorticity is put into the form of Eq. (20) with $\xi = (\Psi_1(r) + cr)\sin\theta$ and $\eta = \mathscr{L}_1\Psi + \beta r\sin\theta$, and a piecewise-linear solution $\eta(\xi)$ is sought.

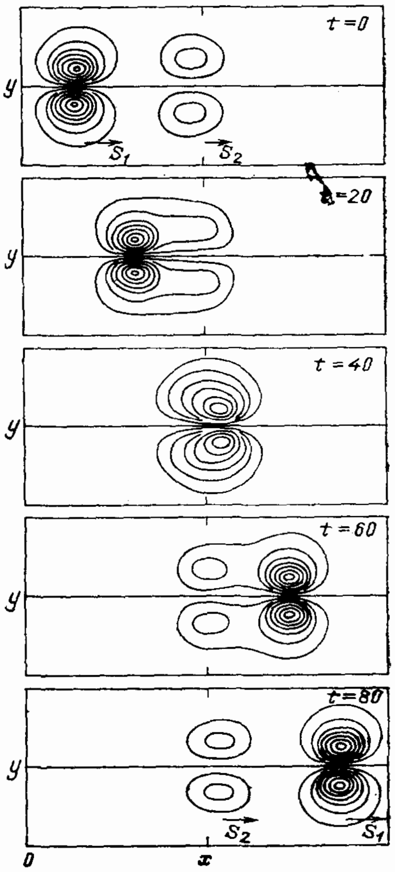

FIG. 19. Passage of one barotropic soliton S_1 through another barotropic soliton S_2 according to the results of numerical experiments by Makino *et al.*[105]

The result is shown in Fig. 20. A three-zone three-dimensional soliton is also constructed in Ref. 108. (it is also shown that, generally speaking, it is impossible to create more than three zones). In three-dimensional solitons some purely radial terms can be added to ψ (but in this case $\partial^2\psi/\partial r^2$. becomes discontinuous).

According to Z. I. Kizner[109,110] the bottom halves of all these three-dimensional solitons satisfy on the surface of the ocean the "solid cover" condition and therefore they can be regarded as autonomous solitons. In these works other three-dimensional solitons are also constructed: $\psi = \psi_0(r,\theta) + \Phi(r)F(z)$, where ψ_0 is a "modon," $F(z)$ is the solution of a Sturm-Liouville problem for the amplitudes of the internal waves, and $\Phi(r)$ are determined differently for $r < a$ and $r > a$. Finally, we mention the solitons

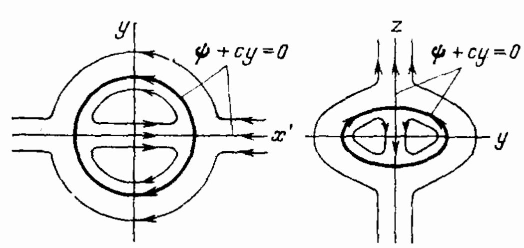

FIG. 20. Three-dimensional soliton of A. L. Berestov.[108]

"trapped" by features of the bottom relief or other localized disturbances of the stream function; such solitons were studied, for example, by A. Patoine and T. Warn,[111] T. Warn and B. Brasnet,[112] and R. Pierrehumbert and P. Malguzzi.[113]

III. MESOSCALE EDDIES

9. "MEZOPOLIGON"

Mesoscale ocean eddies, by definition, have horizontal dimensions $L \gtrsim H$, i.e., from kilometers to tens of kilometers, and periods (Eulerian) from many hours to many days (see Ref. 17). Such eddies were observed during the POLYMODE experiment and in other expeditions, but only occasionally, creating the impression that they are relatively rare formations. To shed light on this question it was necessary to perform a special observational experiment with a tighter network of AFSs.

Such an experiment was performed in the Mezopoligon expedition of the Institute of Oceanography of the Academy of Sciences of the USSR in April–June 1985 in the trade-wind zone of the North Atlantic,[17] where 76 AFSs with 215 flowmeters were deployed over an area 60×80 square miles, and four hydrological surveys were made over a period of 35 days. As a result, both synoptic and mesoscale eddies with diameters ranging from 30 to 50 miles, in which flow velocities reached 20–25 cm/s and which occasionally appeared in zones of tangential velocity shear between neighboring sometimes synoptic eddies of the same sign (apparently arising owing to the Helmholtz instability), were observed. But the main observation was a formation which was dubbed Linza. This formation was traced for three months in eight hydrological surveys, an additional meso-survey area consisting of 16 AFSs, and numerous soundings. This was a lenticular volume of anomalously warm and saline water in a layer between the depths 800 and 1300 m.

In the plane Linza had an oval form with an average diameter of about 30 km and a volume of the order of 10^3 km^3. The well-mixed core of Linza, located in the layer from 960 to 1060 m, was found to contain maximum, for this region of the ocean, anomalies of the temperature and salinity, equal to 4.5 °C and 0.87%. The temperature distribution on the zonal section through the center of Linza is presented in Fig. 21. A region of high hydrostatic stability immediately

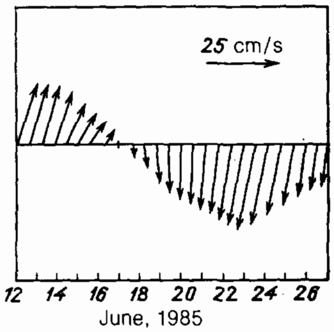

FIG. 22. Vector hodograph of flows at a depth of 1000 m (according to AFS data).

above the core was separated in the density distribution; below this region lay a region of small vertical gradients and above it lay a secondary "superstructure" of mixed waters, which also had small vertical gradients. Six to seven quasiuniform layers separated by secondary pycnoclines can be seen. With time the layers, separated from one another by jumps of the density, through which the waters do not mix readily, probably become increasingly more independent of one another. Thus the aging of Linza is manifested as decomposition into quasiautonomous layers. Based on this it can be conjectured that this Linza is quite old.

The characteristic feature of the density distribution in Linza corresponds completely to anticyclonic eddy motion of waters in it (measured with the help of AFBs), the velocity of which reached 29 cm/s at a depth of 1000 m (Fig. 22). The background large-scale flow transported Linza to the northwest with an average speed of about 2.4 km/day. One can attempt to establish the origin of Linza based on its (T,S) curve, i.e., a graph with the coordinates T and S on which points corresponding to increasing depths are systematically plotted. These (T,S) curves are very different in different regions of the ocean. In Fig. 23 one can see that in the layer 800-1300 m the (T,S) curve in the region of Linza has a very sharp anomaly, making this curve look more like the (T,S) curve for the Mediterranean Sea.[114] This also pertains to the concentration of oxygen, nitrates, phosphorus, and silicon, the pH, and the alkalinity measured in Linza. The

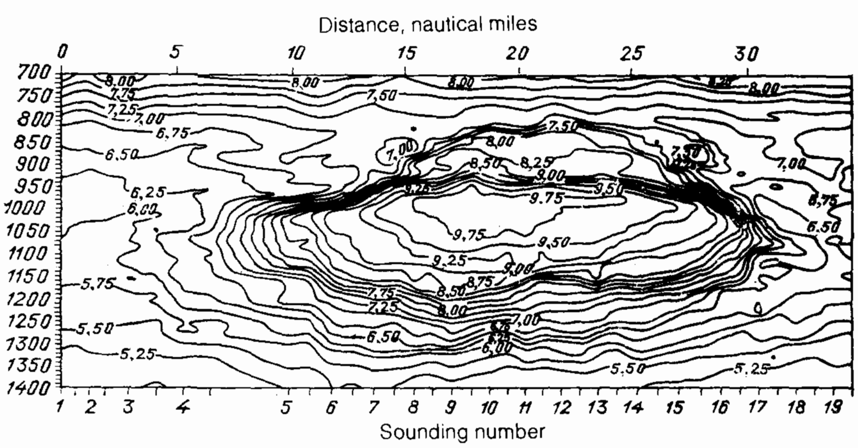

FIG. 21. Temperature distribution in a section through the center of the Mezopoligon lens.

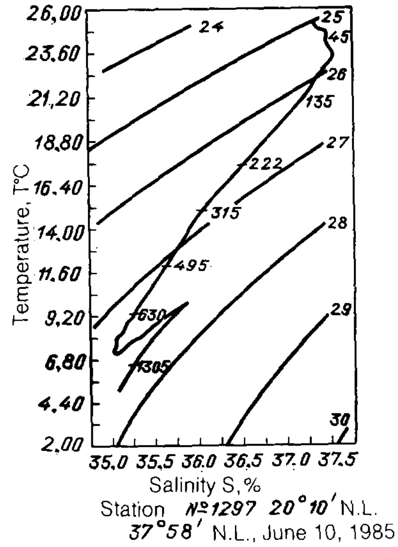

FIG. 23. *T*, *S*-curve at the center of the lens. Station No. 1297 (20° to 10′ N.L., 37°58′ W.L.).

large distance of Linza from the region where it was engendered to the west of the Strait of Gibraltar (about 2500 km) together with the large temperature and salinity anomalies in its core indicate that such eddies are highly stable and they can exist in the ocean for many months and possibly years and traverse distances of thousands of kilometers.

The water flowing out of the Mediterranean Sea is apparently one of the main sources of lenticular formations in the North Atlantic. However the mechanism of lens formation has not yet been established unequivocally. It is possible that lenses arise as a result of instability of a front of intrusive waters analogously to the manner in which meanders of stream flows form and are cut off. Because of their large volume ($\sim 10^3$ km^3, i.e., of the order of the discharge from the Mediterranean Sea through the Strait of Gibraltar over a period of one month) it seems less likely that the lenses formed as discrete portions of water flowing from the Mediterranean Sea under the action of variable wind and/or tides. But lenses could form in the open ocean as a result of isopycnic intrusion of anomalous waters formed on the oceanic shelf.[115]

The discovery of Linza on the "Mezopoligon" once again focused attention on earlier observations of lenses. Lenses were apparently first observed in nature by Soviet oceanographers in the Arctic Basin in the 1930s.[116] Later they were observed in all oceans, but the most detailed studies were performed in the North Atlantic, evidently because of the large number of different scientific expeditions made in this region of the oceans in the 1970s and 1980s. We shall describe several of the most interesting results. Interest in lenses increased significantly after a solitary baroclinic eddy was observed and described in the southwestern part of the Sargasso Sea during the POLYMODE experiment.[117] The lens was concentrated in a layer from 200 to 1400 m and had a diameter of about 100 km. The rotational speed of the water in it reached 20–30 cm/s at a depth of 500-600 m, and neutrally buoyant floats deployed in its core,showed that it drifted over a period of 30 days southwestward with a speed of about 6 cm/sec. In addition, it turned out that the core consisted of water whose hydrophysical characteristics differed markedly from the surrounding waters of the Sargasso Sea and which was similar to waters originating in the Mediterranean Sea. This result suggested that the Mediterranean Sea is a constant source of lenses for the North Atlantic. This hypothesis was later confirmed by the results of more detailed studies performed by L. Armi and W. Zenk.[118] Based on hydrological data, they observed a cluster of three lenses in the region southwestward of the Strait of Gibraltar (the northern part of the Canary Basin). These lenses had well-mixed cores and were separated by distances of 250–500 km from one another. They had diameters of about 100 km and they were concentrated in a layer from 700 to 1500 m. The speed of anticyclonic rotation in them reached 25–30 cm/s. The depth of these lenses as well as the temperature (11.65 °C, the salinity 36.2%), and the density ($\sigma_t \approx 27.69$ g/cm^3) of the mixed waters indicated that these eddies were formed in the region of the Gulf of Cadiz at the outer edge of the layer of waters intruding from the Mediterranean Sea. The saline and warm waters (11–12 °C, 36.3–36.6%, $\sigma_t \approx 27.75$–17.85 g/cm^3), intruding from the Strait of Gibraltar, dropped to a depth of 500–1600 and at first moved westward and then spread out primarily northward. In the opinion of Armi and Zenk these waters are the source for the formation of the lenses, which cover up to 8% of the area of the Canary Basin.

In the seas of the Arctic Basin and in the north Arctic Ocean one of the possible mechanisms of formation of lenses is connected with the intrusion of warm saline waters from the Pacific Ocean through the Bering Strait and from the Atlantic through the Frama Strait (between Greenland and Sptizbergen). Two expeditions in the Frama Strait discovered three lenses with positive temperature and salinity anomalies; these lenses were apparently generated as a result of baroclinic instability of the polar front (T. Manly *et al.*[119]). Most of the lenses in the Arctic were discovered in the Amerasia Basin. P. N. Belyakov and V. A. Volkov[120] analyzed measurements of the flow velocities at the stations "Severnyĭ polyus" in the Chukot-Alaska sector of the Arctic and recorded 350 local increases of the flow velocity at intermediate levels. In many cases they were also able to observe the eddy structure of the circulation. It turned out that the saturation of the ocean with eddies (as with most of the lenses already described) is especially high in the region of high values of the vertical gradient of the water density at the top of the main pycnocline. Results close to those described above were obtained by J. Newton *et al.*[121] and K. Hunkins[122] based on observations with three drifting ice stations in the spring of 1972 in the Beaufort Sea. Measurements of the temperature, salinity, and flow velocity made it possible to record three anticyclonic eddies and one cyclonic eddy, which had a diameter of 15–30 km, and which were concentrated in a layer 30–350 m, and had an orbital velocity of up to 30 cm/s at a depth of about 150 m. Observations over a longer period of time were performed at approximately the same location from four ice stations in the period from April 1975 to April 1976.[123] As a result, a total of 128 lenses, 95 of which were anticyclones, were recorded. Their movements over the area of the sea were determined primarily by large-scale geostrophic flows and their velocities were equal to about 2 cm/s. T. Manly and K. Hunkins[123] conjecture that these eddies are formed as a result of baroclinic instability of a large-scale eastward flow along the edge of the shelf of the northern coast of Alaska and carrying in its upper part water originating in the Pacific Ocean.

The waters of the Red Sea in the Indian Ocean and other anomalous water masses of regional formation, penetrating into definite layers of the ocean through straits or from shelves, should behave analogously. Because of the weakness and intermittency of small-scale oceanic turbulence all these waters can be regarded as poorly intermixing liquids, whose breakup should engender in each region a mesoscale spottiness which is specific to that region and which can be important for a number of theoretical and practical problems. It is obvious that an extensive program of expeditions opens up here.

We already pointed out in the introduction that the quasigeostrophic approximation may not be sufficient to describe adequately mesoscale eddies. At the same time it is well known that the quasisolenoidal approximation, which takes into account terms of a higher order in Ki than does the quasigeostrophic approximation, is sufficient. In the quasisolenoidal approximation the divergence of the velocity of horizontal flow is small—of the order of $(Ki)^2$—compared with the vertical component of the velocity relative to the eddy, and the equation of the potential vorticity assumes the form (3). To determine the relationship between the stream function field and the pressure field we shall employ the equation for the divergence of the horizontal velocity, in which we retain only terms of order $(Ki)^2 f^2$. As a result we obtain the equation of balance for ψ

$$\nabla(f\nabla\psi) + 2J\left(\frac{\partial\psi}{\partial x}, \frac{\partial\psi}{\partial y}\right) = \rho_0^{-1}\Delta p', \tag{21}$$

which is an equation of the Monge-Ampere type well-known in mathematics. In the geostrophic approximation the second term on the left side is small. The equations of the quasisolenoidal approximation (3) and (21) describe slow (with a typical time scale L/U) motions on synoptic scales and mesoscales not only at middle and high latitudes but also in the equatorial region, where the Coriolis parameter f becomes negligibly small (see Refs. 6, 124, and 127 for a more detailed discussion).

10. CTD SCANNING

Aside from lenses in the ocean, an entire spectrum of mesoscale eddies, whose vertical dimensions are many tens and several hundreds of meters and which are concentrated primarily in the main thermocline, is observed in the ocean. These eddies transport water, but the contrasts between the water in their central part (core) and the water mass surrounding the eddy are not as large as in lenses. At the same time, like in the case of lenses, the beta effect in them is weak (owing to the small horizontal scales) and the geostrophic equilibrium between the pressure gradient and the Coriolis force can break down (so that only the quasisolenoidal approximation can be used to describe them).

An entire class of such eddies was discovered in 1986–1987 with the help of CTD scanning,[128,129] i.e., continuous lowerings and raisings of a CTD probe (C,T, and D are, respectively, the electronic conductivity of sea water, the temperature, and the depth) in a layer with depths ranging, say, from 0 to 500–600 m from a vessel moving with a speed of, say, 6 knots. With the probe raised and lowered at a rate of about 1–1.5 m/s the total scanning cycle is completed in 1.5–2 miles (0.2 miles if the scanned layer lies at a depth of 100 m). This increases the horizontal resolution by an order of magnitude over the resolution achievable with the standard hydrological stations deployed every 10–20 miles, and compared with the measurements performed with a towed device at a fixed depth it gives a complete though not completely synchronous (x,z) section of the hydrophysical fields of the ocean.

In Ref. 129 a Mark-III CTD probe manufactured by the Niel Brown Company was employed. The probe measured the electrical conductivity of the water with an accuracy of 5×10^{-3} mS/cm, the temperature with an accuracy of 5×10^{-3} °C, and the pressure with an accuracy of 0.5%, and in addition the gauges were queried with a frequency of 31 s^{-1}, which gave a vertical resolution of several cm. The salinity s, the density ρ, and the vertical velocity of the probe were calculated from the CTD signals and isolines were plotted on $T,S,\rho|_{x,z}$ and $T,S|_{x,\rho}$ graphs (the latter eliminate oscillations of the T and S isolines caused by linear internal waves: in such oscillations δT and δs are proportional to $\delta\rho$).

We shall present a number of results of CTD scanning, obtained on the 13th cruise of the R/V Akademik Mstislav Keldysh of the Academy of Sciences of the USSR in January–April 1987 in the Atlantic. These results were published in a series of papers by A. S. Monin, R. V. Ozmidov, and V. T. Paka.[19]

In the zone of the Canary upwelling near the northwestern coast of Africa the prevailing winds blowing along the coastline generate drift flows which are deflected from the coast by the Coriolis force and carry off the surface waters. This results in a rise at their locations of deep colder and fresher waters, which are separated from the surrounding surface waters by a frontal zone approximately following the

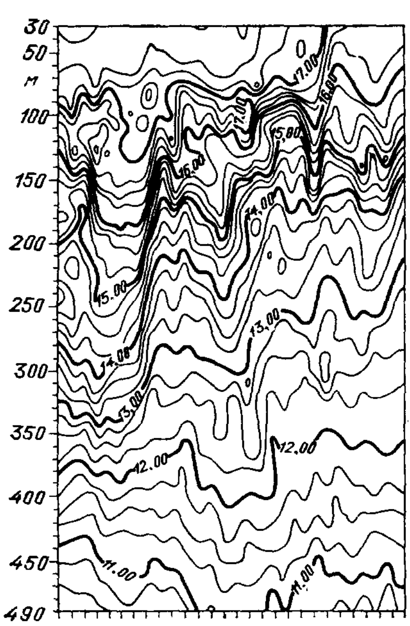

FIG. 24. Canary upwelling. The temperature section through the front.

coastline. The differentials of the temperature and salinity across the frontal region reach 1.3 °C and 0.33%, respectively (V. I. Voĭtov and V. M Zhurbas[130]). Data on the mesostructure of this zone of upwelling have been obtained with the help of CTD scanning. Figure 24 shows a section of the temperature field through a front of upwelling along the parallel 21° N.L. and Fig. 25 shows a section along the coastline in the upwelling waters. The most prominent feature of these sections are sharp oscillations of isothermal surfaces, which trace out "domes" of cold water and "wells" of warm water with diameters ranging from 7–8 to 30–35 km, predominantly at depths of 100–350 m, the total swings of the isothermals reach 100 m and the slope reaches 0.1–0.3. The horizontal temperature gradients in the "walls" of these "domes" and "wells" were of the order of 1 °C/km.

The section along the coastline (Fig. 25) also contained "domes" and "wells," and it was observed that their depth increased from south to north. These nonuniformities of the temperature field in both sections have a quasi-isotropic character and are probably not related with topographical effects, since they were observed primarily in the layer of the upper thermocline. The isohalines in these sections had a completely analogous form, i.e., "domes" and "wells" of relatively fresher and saline waters, respectively, could be seen in them. The fact that the isothermal and isohaline surfaces have approximately the same form the same signs of variations in the temperature and salinity (increase in the "wells" and decrease in the "domes") mainly compensates density variations through the front of upwelling, but on the section along the coast they remained noticeable in the density field also. The largest "well" had a diameter of about 6 km and a depth of about 100 m (marked by an arrow in Fig. 25). The density on its axis was $(0.12–0.15)\sigma_t$ lower than in the surrounding waters. The formation of such "domes" and "wells" is apparently not connected with internal waves. Indeed, the temperature and salinity fields in the sections shown in Figs. 24 and 25 were recalculated using the density σt as the vertical coordinate. The sharp oscillations of the temperature and salinity remained almost unchanged.

These nonuniformities could be caused by the vertical motions w_E generated by the nonuniform and nonstationary Ekman "pumping" in the field of the curl $\nabla \times \tau$ of the tangential wind stress on the ocean surface; see formula (5) in Sec. 2. The hypothesis of forced convection is supported by the asymmetry of the ascending and descending motions: the ascending streams ("domes") are wider and weaker than the descending streams ("wells"). To generate such Ekman pumping the wind-stress field must contain quite developed mesoscale disturbances. They could be "coherent structures" (i.e., least unstable large-scale disturbances), having horizontal dimensions of the order of kilometers, in the atmospheric boundary layer.

An analogous mesostructure was observed in the Mediterranean Sea southward of the Golfe du Lion. The results of sounding are presented in Fig. 26 in the form of a section in the temperature field of the upper 490-m layer. During the observations winter-spring convection, which is quite rare during this season and which extended to depths of 2–2.5 km (to the bottom), occurred; this convection destroyed the mesostructure of the upper layer and resulted in the formation of mixed waters with a temperature of about 12.8 °C, salinity of 38.45%, and nominal density of 29.11, situated on the left side of the section. However behind the convection front, across which the temperature differentials equaled about 0.3 °C and the salinity differentials equaled about 0.05%, the mesostructure remained (the right side of the section). It had the same shape of "domes," "wells," and "drops" of relatively cold and warm waters in the layer from the surface to depths of 300–350 m.

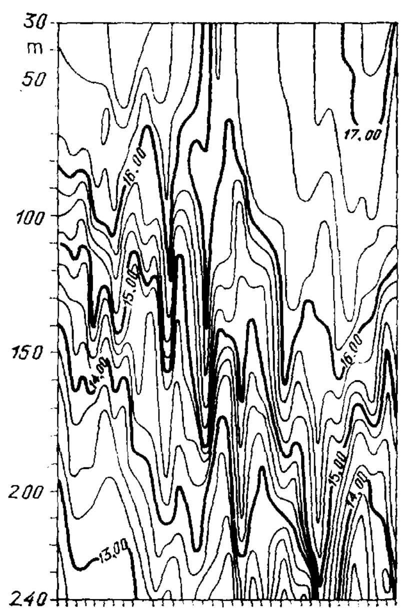

FIG. 25. Canary upwelling. Temperature section along the shore.

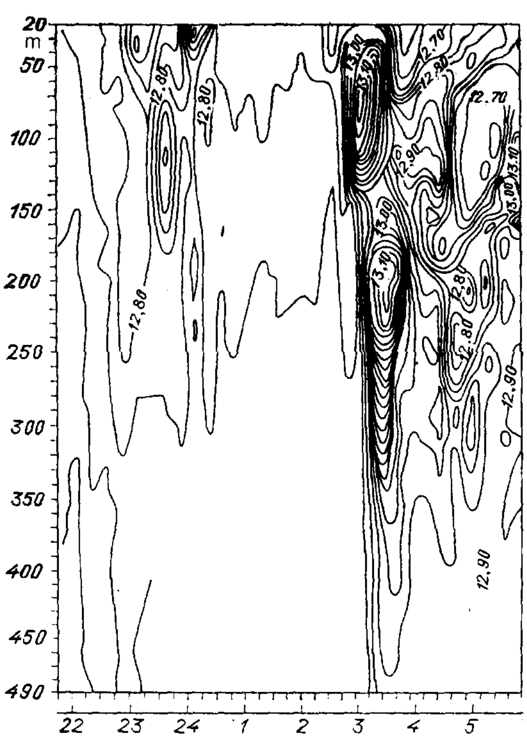

FIG. 26. Convection in the Mediterranean Sea.

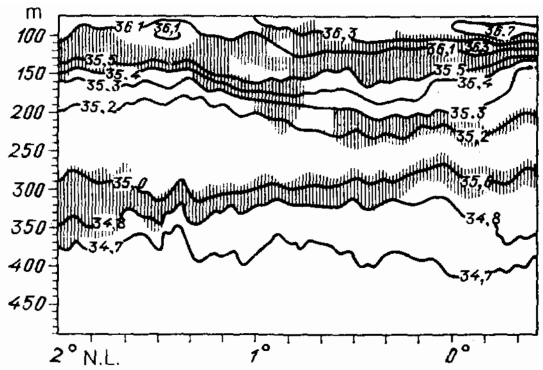

FIG. 28. Equatorial mesostructure. Section of the salinity field.

A well-resolved mesostructure was discovered in the region of the underwater mountain Ampere, located approximately 400 miles west of the Strait of Gibraltar and rising above the surrounding bottom to a height of 2.5 km (the summit lies at a depth of 65 m). On meridional sections west of the summit the mesostructure in the layer 20–200 m included alternation of relatively wide "domes" of cold and fresher water and "wells" of warm and saline water. The variations of the temperature and salinity did not compensate one another, and analogous fluctuations were observed in the density field (repeated sounding every 4.5 h gave the same mesostructure). Measurements on AFSs revealed a general flow from the northwest to the southeast with a strong semidiurnal tidal component superposed on it. A hodograph of the flow velocities showed that over a period of about two days the flow revolved around the mountain four times; in addition, the flow weakened to the northwest and intensified to the southwest (the quasistationary general flow was added to the nonstationary tidal flow). It is obvious that the wake of the flow past the mountain should revolve around the mountain in the same manner; this should introduce a nonstationary periodic component into the usual mesostructure of the main thermocline.

The wake behind the mountain was observed in the CTD section to the southwest of the mountain. The observations at depths of 30–80 m are presented in Fig. 27. One can see in the temperature section of Fig. 27 that the wake is manifested against the background of the irregular mesostructure in the form of a cold "dome" above a warm "well" with almost vertical sharp walls. The "hyperbolic point" separating these disturbances was located at a depth of 65 m, i.e., at the level of the summit; in Fig. 27 this point lies on the axis of the wake. In the section of the salinity field the wake had an analogous form with respect to the fresh water "dome" above the saline "well," "squeezed" between two wider "domes." The variations of the salinity and temperature did not compensate one another, and the wake was also clearly manifested in the water-density field. In the section of the nominal density field the wake had the form of a sharp "dome" of dense water above a "well" of moderate density, separated by an isopycnal near $\sigma_t = 26.585$ and squeezed between two wide "wells" of low-density waters.

This section shows clearly that the wake is formed as a result of the rising of dense deep waters on the windward slope of the mountain, which is compensated by sinking on both sides of the wake. This sinking can apparently engender two cylindrical or "roll" eddies whose horizontal axes are quasiparallel to the wake; judging from Fig. 27, underneath these eddies there are apparently eddies with the opposite rotation, possibly induced by the upper eddies—then these induced eddies explain the "well" below the "hyperbolic point." Recalculation of the temperature and salinity sections using σ_t as the vertical coordinate made it possible to eliminate the effect of internal gravity waves and separate some features of the mesostructure of the fields of the upper layer. Such a section of the temperature field shows that the mesostructure in the region of Mt. Ampere is not caused by linear internal waves. Two wide "domes" of cold, fresher, deep waters, separated by the warm and saline "wells," as well as finer details (owing to some "stretching" of the isolines in the new frame of reference) can be seen on them. We note that instead of the "dome" of deep water lying above the "hyperbolic point" in Fig. 27 between the warm and saline "wells" the opposite, compensational picture was observed in the coordinate σ_t. The "well," however, did not correspond completely to the wake, whose axis lay on the left slope of the "well"; it is possible that this asymmetry is connected with the nonstationary nature of the wake—clockwise rotation together with the tidal flow.

Since the wake, described above, behind the mountain is obviously not formed by internal waves, but, apparently, rotates, it seems that it can be approximately regarded as resulting primarily from the transport of quasigeostropic baroclinic potential vorticity above the mountain in the f-plane approximation. Such dynamics, together with the superposed tidal flow, greatly complicates the overall mesoscale pattern of the flows. This pattern could have a nonperiodic character and requires both additional field data and mathematical and laboratory modeling for a more detailed study.

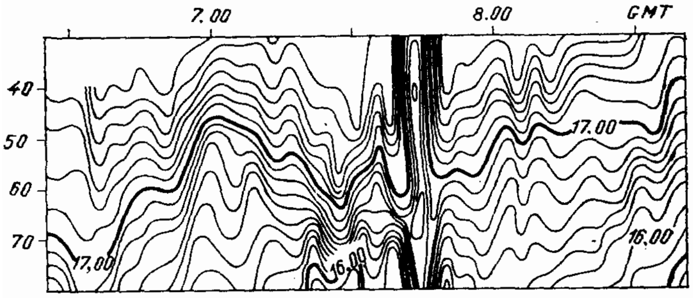

FIG. 27. Water area around Mt. Ampere. Section of the temperature field.

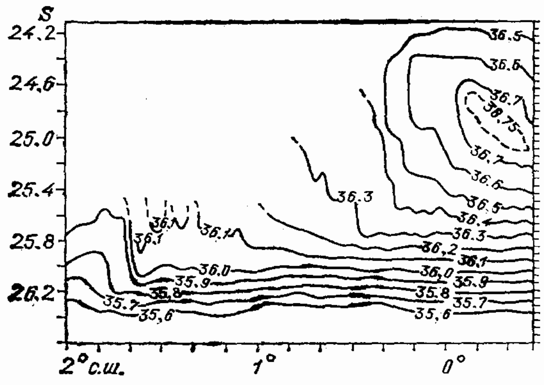

FIG. 29. Equatorial mesostructure. Salinity in σ_t coordinates.

The unique layered mesostructure of the upper layer of the ocean was discovered in two other regions of the ocean. In the first case we are talking about data obtained on the meridional section through the equator in the Atlantic Ocean along 35° W.L. from 2° N.L. to 0° 26′ S.L. An interesting object in the section was the equatorial subsurface current, in the Atlantic called the Lomonosov current, which is best separated in the salinity data. For this reason a section in the salinity field was employed to analyze the mesostructure. In the section presented in Fig. 28 the salinity almost everywhere decreases with depth—on the average from values of about 36.4% at the surface of the ocean to 34.7% at a depth of 400 m. The section demonstrates an unusual pattern of three haloclines: the top halocline lies at depths of about 100–150 n, the middle halocline occurs only in the right half of the section at depths of 200–230 m, and the bottom halocline lies on the average at depths of 280–310 m and its southern part is substantially expanded. The overall pattern of the stretchings, compressions, and inclinations of the isohalines is reminiscent of the bellows of an accordion and suggests that internal waves played a significant role in its formation. The section in the temperature field has an analogous appearance, the only difference being that the Lomonosov current is not distinguished (in Fig. 28 it is bounded by the 36.5% isohaline).

Figure 29 shows the salinity section in the vertical coordinate σ_t. A new nonisopycnal mesostructure of the upper layer appears in it. This is, first of all, the Lomonosov current and, second, a very sharp salinity front at 1° 4′ N.L. with a horizontal salinity differential from 35.5–35.9 to 36.1%.

In conclusion we shall present data obtained on sections through the polar front in the North Atlantic during the 48th cruise of the R/V of the Academy of Sciences of the USSR Akademik Kurchatov in March 1988 (N. N. Golenko *et al.*[131]). The survey area was located in the Newfoundland zone (see inset in Fig. 30). The front passed from the southwest to the northeast, separating the warm and saline waters of the North Atlantic current and the cold and slightly fresher Labrador waters. One can see from Fig. 30 that the front meanders strongly, forming warm meanders with axes directed northward ("crests" in the field of the surface tem-

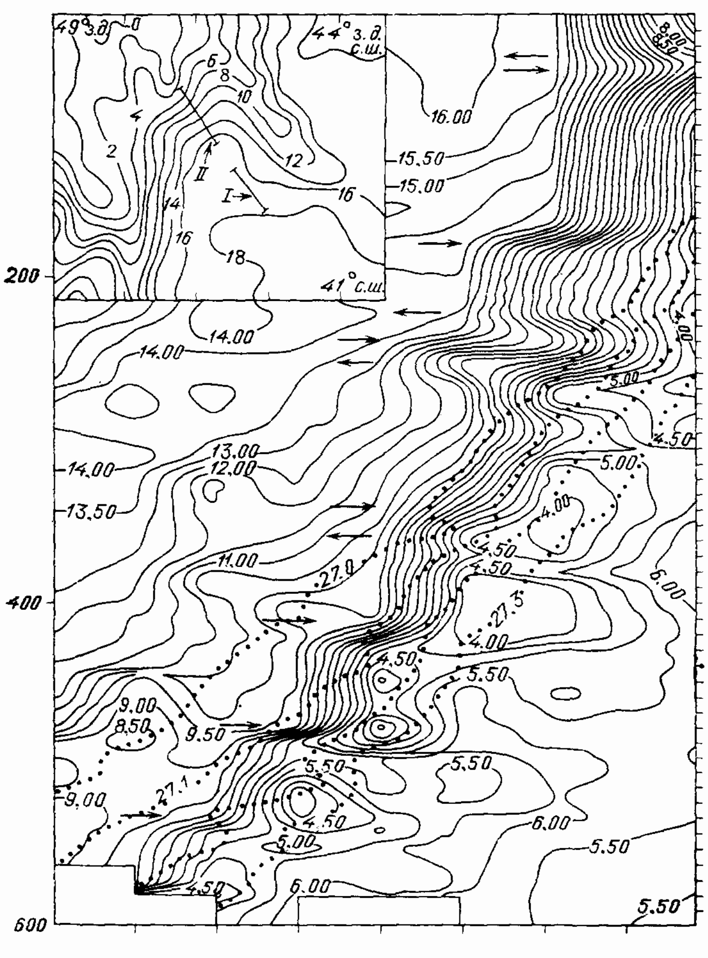

FIG. 30. Polar front. Section of the temperature field and facsimile map (inset).

perature of the ocean), and cold meanders ("troughs"). The section in the temperature field was made through the warm meander approximately along its axis. The front is inclined from north to south with an angle of inclination of about 0.5°, and in addition its thickness and intensity decrease with depth. The temperature differentials across the front are partially compensated by opposite differentials of the salinity, and the nominal density increases comparatively smoothly from 26.5 at small depths in the southern waters to 27.5 at great depths in the northern waters; in addition, the front, more precisely, the cold subfrontal waters, correspond to the interval of nominal density 27.2–27.3 (see Fig. 30, where the circles depict the isopycnics).

The slope of the frontal surface and the general arrangement of the warm masses above the cold masses are the same as in the case of atmospheric fronts. However the oceanic front is distinguished by two features: first, the arrangement of the cold waters themselves (temperatures of 3.5–4.5 °C) with the lowest salinity (34.2–32.4%) directly beneath the frontal zone and above the slightly warmer and saline waters (5–6 °C, 34.6–34.9%) and, second, the splitting of the frontal zone along the vertical into quasiuniform layers 50-100 m thick, separated by thin vertical interlayers with large vertical temperature gradients, where the temperature either increases or decreases with depth. Such microthermoclines are indicated in Fig. 30 by arrows, oriented to the right when the temperature in them decreases and to the left when the temperature increases. In the latter case temperature intervals occurred, the most significant of which were located at depths of 260–280 m.

The first feature is apparently connected with the isopycnic intrusion of cold and dense ($\sigma_t = 27.2$–27.3) Labrador surface waters into the mass of inflowing warm and saline waters of the North-Atlantic current. The second feature—splitting, on the average, of the inclined frontal zone—indicates its unique instability, a tendency of the warm waters to move northward in comparatively thick quasiuniform and sometimes even temperature-inverted layers along thin quasiisopycnic interlayers. The stratification also encompasses the subfrontal cold intrusion, seemingly dividing it into separate portions; however, this impression is weakened somewhat if the density is employed as the vertical coordinate instead of the depth. These two features apparently represent the same dynamical process of intrusion of water masses into the ocean, which is accompanied by formation of layered mesoscale structures with vertical sizes of up to 100–150 m. In addition, instabilities and eddy structures can develop. The portions of intrusion of Labrador waters, which in Fig. 30 form "drops" in the bottom half of the subfrontal layer, could be such structures.

The data, presented in this section, on the mesoscale nonuniformities in the ocean are the first results obtained with the help of CTD scanning. Continuation of these studies in ocean expeditions could lead to new discoveries.

[1]H. von Helmholtz, Crelle's J. **55** (1858).

[2]A. A. Fridman, *Experiments in the Hydromechanics of Compressible Fluids* [in Russian], Leningrad, 1934.

[3]A. V. Tur and V. V. Yanovskiĭ, Preprint, Institute of Space Research of the Academy of Sciences of the USSR, Moscow (1989).

[4]A. S. Monin *Theoretical Principles of Geophysical Hydrodynamics* [in Russian], Gidrometeoizdat, Leningrad (1988).

[5]A. S. Monin and R. V. Ozmidov, *Turbulence in the Ocean*, Reidel, Dordrect, 1985 [Russ. original, Gidrometeoizdat, L., 1982].

[6]A. S. Monin, *Weather Forecasting as a Problem in Physics*, MIT Press, Cambridge, Mass., 1972 [Russ. original, Nauka, 1969].

[7]G. I. Marchuk and A. S. Sarkisyan, *Mathematical Modeling of the Circulation of the Ocean* [in Russian], Nauka, M., 1988.

[8]Oceanology, Physics of the Ocean [in Russian], Nauka, M., 1979, Vol. 1.

[9]V. M. Kamenkovich, M.N. Koshlyakov, and A. S. Monin, *Synoptic Eddies in the Ocean*, Reidel, Dordrecht, Boston, 1986 [Russ. original, Gidrometeoizdat, Leningrad, 1982; 2nd ed. 1987].

[10]A. P. Mirabel' and A. S. Monin, Dokl. Akad. Nauk SSSR **303**, 976 (1988) [Dokl. Earth Sci. (1988)].

[11]A. P. Mirabel' and A. S. Monin, *Ibid.* **309**, 716 (1989) [Dokl. Earth Sci. (1989)].

[12]V. A. Bubnov, Yu. A. Ivanov, M. N. Koshlyakov, V. G. Kort, A. S. Monin, and I. M. Ovchinnikov, *Ibid.* **301**, 1468 (1988) [Dokl. Earth Sci. (1988)].

[13]V. E. Zakharov and L. I. Piterbarg, *Ibid.* **295**, 86 (1987 [Sov. Phys. Dokl. **32**, 560 (1987)].

[14]A. S. Monin and L. I. Piterbarg, *Ibid.*, 712 [Dokl. Earth Sci. (1987)].

[15]V. E. Zakharov, A. S. Monin, and L. I. Piterbarg, *Ibid.*, 1061 [Sov. Phys. Dokl. **32**, 626 (1987)].

[16]A. J. Semtner and R. M. Chervin, J. Geophys. Res. C **93**, 15502 (1988).

[17]Yu. A. Ivanov, V. G. Kort, A. S. Monin, I. M. Ovchinnikov, and I. F. Shadrin, Dokl. Akad. Nauk SSSR **289**, 706 (1986) [Dokl. Earth. Sci. (1986)].

[18]A. P. Berestov *et al.* in *Intrathermocline Eddies in the Ocean* [in Russian], edited by K. N. Fedorov, Institute of Oceanography of the Academy of Sciences of the USSR, Moscow, 1986, p. 35.

[19]A. S. Monin, R. V. Ozmidov, and V. T. Paka, Dokl. Akad. Nauk SSSR **297**, 706, 1469 (1987); **298**, 721; **308**, 192 (1989) [Dokl. Earth Sci. (1987); (1989)] Izv. Akad. Nauk SSSR, Fiz. Atmos. Okeana **25**, 1308 (1989) [Izv. Acad. Sci. USSR Atmos. Oceanic Phys. **25**, (1989)].

[20]V. M. Kamenkovich, *Principles of Ocean Dynamics* [in Russian], Gidrometeoizdat, L., 1973.

[21]A. S. Monin, *Introduction to the Theory of Climate* [in Russian], Gidrometeoizdat, L., 1982.

[22]C. H. B. Priestley, Ass. Intern. de Meteorologie, Brussels (1951).

[23]A. M. Il'in and V. M. Kamenkovich, Dokl. Akad. Nauk SSSR **150**, 1274 (1963) [Dokl. Earth Sci. **150**, 9 (1965)].

[24]D. W. Moore, Deep-Sea Res. **10**, 735 (1963).

[25]G. R. Batchelor, J. Fluid Mech. **1**, 177 (1956).

[26]P. Rhines and W. Young, *Ibid.* **122**, 347 (1982).

[27]P. Rhines and W. R. Holland, Dynam. Atmos. Ocean **3**, 285 (1979).

[28]S. McDowell, P. Rhines, and T. Keffer, J. Phys. Oceanogr. **12**, 1417 (1982).

[29]E. T. Eady, Tellus **1**, 33 (1949).

[30]J. Pedlosky, *Ibid.* **16**, 12 (1964).

[31]V. E. Zakharov, Dokl. Akad. Nauk SSSR **228**, 1314 (1976) [Sov. Phys. Dokl. **21**, 322 (1976)].

[32]H. Stommel, The Gulf Stream. *A Physical and Dynamical Description*, Univ. of California (1965), 2nd edition.

[33]F. C. Fuglister and L. V. Worthington, Tellus **3**, 1 (1951).

[34]A. S. Monin and K. N. Fedorov, Dokl. Akad. Nauk SSSR **270**, 1213 (1983) [Dokl. Earth Sci. (1983)].

[35]J. C. Swallow, Philos. Trans. R. Soc. London A **270**, 451 (1971).

[36]K. Wyrtki, Deutsch. Hydr. Zs. **20**, 176 (1967).

[37]V. B. Shtokman, M. N. Koshlyakov, R. V. Ozmidov *et al.*, Dokl. Akad. Nauk SSSR **186**, 1070 (1969) [Dokl. Earth Sci. **186**, 17 (1970)] Sci. USSR Atmos. Oceanic Phys. **20**, 689 (1984).

[38]T. G. Sazhina, Izv. Akad. Nauk SSSR, Fiz. Atmos Okeana **20**, 776 (1984).

[39]L. M. Brekhovskikh, M. N. Koshlyakov, K. N. Fedorov *et al.*, Dokl. Akad. Nauk SSSR **198**, 1434 (1971) [Dokl. Earth Sci. **198**, 249 (1972)].

[40]M. N. Koshlyakov, Okeanologiya **13**, 760 (1973).

[41]V. M. Kamenkovich and G. M. Reznik, Physics of the Ocean, Vol. 2. Hydrodynamics of the Ocean [in Russian], Nauka, M., 1978, Ch. 7.

[42]J. C. McWilliams, J. Phys. Oceanogr. **6**, 810 (1976).

[43]V. N. Drozdov, A. S. Monin, and I. G. Yushina, Dokl. Akad. Nauk SSSR **258**, 331 (1981) [Dokl. Earth Sci. (1981)].

[44]Yu. M. Grachev, M. N. Koshlyakov, and Yu. G. Mikhaĭlichenko, *Synoptic Vortices in the Sargasso Sea* [in Russian], Nauka, M., 1988.

[45]A.D. Buris, V. M. Kamenkovich, and A. S. Monin [Eds.], Atlas POLYMODE, WHOI Contribution No. 6077 (1986).

[46]S. B. Borisov and A. S. Monin, Dokl. Akad. Nauk SSSR **306**, 1230 (1989) [Dokl. Earth Sci. (1989)].

[47]I. A. Bulis and A. S. Monin, *Ibid.* **221**, 597 (1975) [Dokl. Earth Sci. (1975)].

[48]K. Wyrtki, L. Magaard, and J. Hager, J. Geophys. Res. **81**, 2641 (1976).

[49]J. Pedlosky, Geophysical Fluid Dynamics, Springer Verlag, N.Y., 1979, 2nd ed. 1987 [Russ. transl., Mir, M., 1984].
[50]G. M. Zhikharev, Izv. Akad. Nauk SSSR, Fiz. Atmos. Okeana **26** (1990) [Izv. Acad. Sci. USSR Atmos. Oceanic Phys. **26** (1990)].
[51]J. G. Charney and G. R. Flierl, *Evolution of Physical Oceanography*, edited by B. A. Warren and C. Wunsch, MIT Press, Cambridge, Mass., 1981, p. 504.
[52]A. Buzzi, A. Trevisan, and A. Speranza, J. Atmos. Sci. **41**, 637 (1984).
[53]P. B. Rhines and F. Bretherton, J. Fluid Mech. **61**, 583 (1973).
[54]P. B. Rhines, Geophys. Fluid Dynam. **1**, 273 (1970).
[55]N. G. Hogg, GARP Publ. Ser. **23**, 167 (1980).
[56]E. Kalnay-Rivas and L. O. Merkine, J. Atmos. Sci. **38**, 2077 (1981).
[57]H. E. Huppert and K. Bryan, Deep-Sea Res. **23**, 655 (1976).
[58]J. Verron, Geophys. Astrophys. Fluid Dynam. **35**, 257 (1986).
[59]P. L. Richardson, J. Mar. Res. **38**, 673 (1980).
[60]L. Magaard, J. Phys. Oceanogr. **7**, 359 (1977).
[61]J. Willebrand, *Ibid.* **8**, 1080 (1978).
[62]C. Frankignoul and P. Muller, *Ibid.* **9**, 104 (1979).
[63]A. E. Gill, J. S. Green, and A. J. Simmons, Deep-Sea Res. **21**, 499 (1974).
[64]A. S. Sarkisyan, a) *Numerical Analysis and Forecasting of Ocean Currents* [in Russian], Gidrometeoizdat, Leningrad (1977); b) *The Sea: Ideas and Observations on Progress in the Study of the Seas. 6: Marine Modelling*, edited by E. D. Goldberg, I. N. McCave, J. J. O'Brien, and J. H. Steele, Wiley Interscience, N. Y., 1977, p. 363.
[65]K. Bryan, S. Manabe, and R. C. Pacanowski, J. Phys. Ocean. **5**, 30 (1975).
[66]K. Bryan and L. Levis, J. Geophys. Res. **84**, 2503 (1979).
[67]A. S. Monin, Dokl. Akad. Nauk SSSR **200**, 91 (1971) [Dokl. Earth Sci. **200**, 3 (1972)].
[68]F. Webster, Tellus **17**, 239 (1965).
[69]V. P. Starr, Physics of Negative Viscosity Phenomena, McGraw-Hill, N.Y., 1968 [Russ. transl., Mir, M., 1971].
[70]R. V. Ozmidov, V. S. Belyaev, and A. D. Yampol'skiĭ, Izv. Akad. Nauk SSSR, Fiz. Atmos. Okeana **6**, 285 (1970) [Izv. Acad. Sci. USSR Atmos. Oceanic Phys. **6**, 160 (1970)].
[71]A. S. Monin and D. G. Seidov, Dokl. Akad. Nauk SSSR **268**, 454 (1983) [Dokl. Earth Sci. (1983)].
[72]G. P. Williams and D. R. Davis, Quart. J. Roy. Meteorol. Soc. **91**, 471 (1965).
[73]W. R. Holland and L. B. Lin, J. Phys. Oceanogr. **5**, 658 (1975).
[74]W. R. Holland, *Ibid.* **8**, 363 (1978).
[75]P. Rhines, J. Fluid Mech. **69**, 417 (1975).
[76]P. Rhines in: Ref. 64b, p. 189.
[77]G. K. Batchelor, Phys. Fluids Suppl. II **12**, 233 (1969).
[78]D. G. Seidov, Izv. Akad. Nauk SSSR, Fiz. Atmos. Okeana **14**, 757 (1978); **16**, 73 (1980) [Izv. Acad. Sci. USSR **16**, Atmos. Oceanic Phys. **14**, 538 (1978); **16**, 46 (1980)].
[79]D. G. Seidov, A. D. Marushkevich, and D. A. Nechaev, Okeanologiya **26**, 885 (1986); Dokl. Akad. Nauk SSSR **289**, 980 (1986) [Dokl. Earth Sci. (1986)].
[80]V. E. Zakharov and E. A. Kuznetsov, Preprint No. 185, Institute of Atomic Energy, Siberian Branch of the Academy of Sciences of the USSR, Novosibirsk, 1983.
[81]A. Veĭnsteĭn, Phys. Fluids **26**, 388 (1983).
[82]K. Kenyon, in *Notes on the 1964 Summer Study Program in Geophysical/Fluid Dynamics at the Woods Hole Oceanographical Institute: Student Lectures* (1964), Vol. 2, p. 69.
[83]M. Longuet-Higgins and A. E. Gill, Proc. R. Soc. London A **299**, 120 (1967).
[84]G. M. Reznik, Int. J. Nonlinear Mech. **19**, 95 (1984).
[85]G. M. Reznik and T. E. Soomere, Okeanologiya **24**, 373 (1984).
[86]M. V. Nezlin, Usp. Fiz. Nauk **150**, 3 (1986) [Sov. Phys. Usp. **29**, 807 1986].
[87]L. G. Redecopp, J. Fluid Mech. **82**, 725 (1977).
[88]D. L. T. Andersen and P. D. Killworth, Deep-Sea Res. **26**, 1033 (1979).
[89]V. I. Petviashvili, Pis'ma Zh. Eksp. Teor. Fiz. **32**, 632 (1980) [JETP Lett. **32**, 619 (1980)].
[90]P. M. Rizzoli and M. C. Hendershott, Dynam. Atmos. Oceans **4**, 247 (1980).
[91]T. Matsuura and T. Yamagata, J. Phys. Oceanogr. **12**, 440 (1982).
[92]G. P. Williams and T. Yamagata, J. Atmos. Sci. **41**, 453 (1984).
[93]G. P. Williams, *Ibid.* **42**, 1237 (1985).
[94]G. G. Sutyrin, Dokl. Akad. Nauk SSSR **280**, 1101 (1985) [Dokl. Earth Sci. (1985); Izv. Akad. Nauk SSSR, S. Mekh. Zhidk. Gaza **4**, 119 (1985) [Fluid Dynamics (1985)]; G. G. Sutyrin and I. G. Yushina, Dokl. Akad. Nauk SSSR **288**, 585 (1986) [Dokl. Earth Sci. (1986)].
[95]Yu. A. Danilov and V. I. Petviashvili, *Progress in Science and Technology. Series on Plasma Physics* [in Russian], edited by V. D. Shafranov, VINITI, Academy of Sciences of the USSR, Moscow (1983), No. 4, p. 5.
[96]R. A. Antonova, V. P. Zhvaniya, D. G. Lominadze, D. I. Nonabashvili, and V. I. Petviashvili, Pis'ma Zh. Eksp. Teor. Fiz. **37**, 545 (1983) [JETP Lett. **37**, 651 (1983)]; V. I. Petviashvili and V. V. Yan'kov, Rev. Plasma Phys. **14**, 1 (1989) [Russ. original, Voprosy teoriiplazmy, Ėnergoatomizdat, M., **14**, 3 (1985)].
[97]G. S. Golitsyn, Icarus **13**, 1 (1970).
[98]A. L. Berestov and A. S. Monin, Usp. Mekh. **3**, 3 (1980).
[99]H. Lamb, *Hydrodynamics*, 6th ed., Cambridge Univ. Press, 1932 [Russ. transl., Gostekhizdat, M., 1947].
[100]M. Stern, J. Mar. Res. **33**, 1 (1975).
[101]V. D. Larichev and G. M. Reznik, Dokl. Akad. Nauk SSSR **231**, 1077 (1976) [Dokl. Earth Sci. (1976)].
[102]V. A. Gordin and V. I. Petviashvili, *Ibid.* **285**, 857 (1985) [Sov. Phys. Dokl. **30**, 1004 (1985)].
[103]R. E. Davis and A. Acrivos, J. Fluid Mech. **29**, 593 (1967).
[104]V. D. Larichev and G. M. Reznik, Dokl. Akad. Nauk SSSR **264**, 229 (1982) [Dokl. Earth Sci. (1982)].
[105]M. Makino, T. Kamimura, and T. Taniuti, J. Phys. Soc. Jpn. **50**, 984 (1981).
[106]G. Flierl, in *Investigations of the Synoptic Variability of the Ocean. Proceedings of the Soviet-American Institute POLYMODE, Yalta, 1976*, edited by A. S. Monin and B. A. Nelepo, Marine Hydrophysical Institute of the Academy of Sciences of the Ukrainian SSR, Sevastopol', p. 373.
[107]G. R. Flierl, V. D. Larichev, J. C. McWilliams, and G. M. Reznik, Dyn. Atmos. Ocean **5**, 1 (1980).
[108]A. L. Berestov, Izv. Akad. Nauk SSSR, Fiz. Atmos. Okeana **15**, 648 (1979). [Izv. Acad. Sci. USSR Atmos. Oceanic Phys. **15**, 443 (1979)].
[109]Z. I. Kizner, in *Abstracts* (in Russian) *of Reports at the 2nd All-Union Symposium*, Tallin (1984), Part II, p. 19.
[110]Z. I. Kizner, *Ibid.*, p. 22; Dokl. Akad. Nauk SSSR **275**, 1495 (1984) [Dokl. Earth Sci. (1984)].
[111]A. Patoine and T. Warn, J. Atmos. Sci. **39**, 1018 (1982).
[112]T. Warn and B. Brasnet, *Ibid.* **40**, 28 (1983).
[113]R. Pierrehumbert and P. Malguzzi, *Ibid.* **41**, 246 (1984).
[114]E. A. Plakhin, *Hydrology of Inland Seas* [in Russian], Gidrometeoizdat, Leningrad, 1989.
[115]L. H. N. Cooper, Oceanography, AAAS, Washington (1961), p. 599.
[116]P. P. Shirshov, Dokl. Akad. Nauk SSSR **19**, 569 (1938) not transl.
[117]S. E. McDowell and H. T. Rossby, Science **202**, 1085 (1978).
[118]L. Armi and W. Zenk, J. Phys. Oceanogr. **14**, 1560 (1984).
[119]T. Manly *et al.*, Europ. Ocean. Soc. **62**, 627 (1982).
[120]P.N. Belyakov and V. A. Volkov, Dokl. Akad. Nauk SSSR **254**, 752 (1980) [Dokl. Earth Sci. (1980)].
[121]J. Newton, K. Agaard, and L. Coachman, Deep-Sea Res. **21**, 707 (1974).
[122]K. Hunkins, *Ibid.*, 1017.
[123]T. Manly and K. Hunkins, J. Geophys. Res. C **90**, 4911 (1985).
[124]A. S. Monin, Izv. Akad. Nauk SSSR, Fiz. Zemli, No. 4, 76 (1952); No. 4, 497 (1958).
[125]J. G. Charney, in *Proceedings of the International Symposium on Numerical Weather Prediction*, Met. Soc. Jpn., Tokyo (1962).
[126]B. Bolin, Tellus **7**, 27 (1955).
[127]P. D. Thompson, J. Meteorol. **13**, 251 (1956).
[128]R. Pollard, Nature **323**, 433 (1986).
[129]R. V. Ozmidov, Okeanologiya **28**, 182 (1988).
[130]V. I. Voĭtov and V. M. Zhurbas, *Physical and Oceanographic Studies in the Tropical Atlantic* [in Russian], Nauka, M., 1986, p. 112.
[131]N. N. Golenko, A. S. Monin, and R. V. Ozmidov, Dokl. Akad. Nauk SSSR **309**, 1207 (1989) [Dokl. Earth Sci. (1989)].

Translated by M. E. Alferieff